Scientific Research Publishing

Advances in Bioscience and Biotechnology, 2025, 16(2), 30-64
https://www.scirp.org/journal/abb
ISSN Online: 2156-8502
ISSN Print: 2156-8456

Centrosomes and Not-Coding DNA during the Emergence and Evolution of Bilaterally Symmetric Complex Organs: Computational Models

Marco Franco Giulio Regolini

Department of Biophysics, MFR Bioengineering, Milano, Italy
Email: m.regolini@libero.it

How to cite this paper: Regolini, M.F.G. (2025) Centrosomes and Not-Coding DNA during the Emergence and Evolution of Bilaterally Symmetric Complex Organs: Computational Models. *Advances in Bioscience and Biotechnology*, **16**, 30-64.
https://doi.org/10.4236/abb.2025.162003

Received: December 19, 2024
Accepted: February 15, 2025
Published: February 18, 2025

Abstract

The origin of complex biological symmetric structures has long been a subject of interest and debate. How new sophisticated structures arise, perfectly meshed together, and added to preexisting organs without breaking their anatomy and physiology remains challenging. A mystery is how endless amounts of new bilaterally symmetric organs have arisen in an infinite number of species: bilateral symmetry requires two different pathways for arranging and driving cells in symmetric locations in the left and right halves of the organism. It is unsustainable that two different genetic codes, independent of each other and assembled by chance, have simultaneously arisen for every organ in millions of different species. Many findings have evidenced that DNA tandem repeats and centrosomes are involved in morphogenesis, suggesting they have played a role in the evolution of shapes. This paper introduces computational simulations to test and ascertain whether DNA tandem repeats and centrosomes can manage and accelerate the evolution of complex organs and bilaterally symmetric structures. The present study follows an interdisciplinary perspective that combines biology and computational modeling to understand cellular behavior across species, underlying the similarity between programming and cellular procedures. The integration of programming codes, tandem repeats, centrioles, and centrosomes provides a potential framework for investigating fundamental biological processes.

Keywords

Symmetry, Chirality, Enantiomorphism, Satellite DNA, Tandem Repeats

1. Warning

1) *Does evolutionary theory need a rethink*?

Canonical evolutionary theory fits well with microevolution: the evolution of resistance, pests to pesticides, weeds to herbicides, and pathogens to antibiotics. However, it encounters some difficulties in dealing with macroevolution, the evolution of complex, bilaterally symmetric organs. At this point, caution must be exercised.

The mere mention of new ideas on evolution evokes an emotional, even hostile, reaction among evolutionary biologists: too often, vital discussions descend into acrimony, with accusations of muddle or misrepresentation. Perhaps haunted by the specter of intelligent design, evolutionary biologists wish to show a united front to those hostile to science. However, without an extended evolutionary framework, the theory neglects key processes [1].

Classical evolutionary theory was founded on natural selection, ignoring the existence of genes, but it has now come to focus almost exclusively on genetic inheritance and processes that change gene frequencies.

If it could be demonstrated that any complex organ existed, which could not possibly have been formed by numerous, successive, slight modifications, my theory would absolutely break down said Darwin, and confessed that it is *absurd* to propose that *the human eye evolved through spontaneous mutations and natural selection. It seems, I freely confess, absurd in the highest possible degree. The eye to this day gives me a cold shudder*, he wrote to a friend.

Nowadays, computational models are powerful tools to shed light on this topic.

2) *Computational models*

Given the structure of an experiment, it may not be possible to perform it. Computational models allow us to simulate experiments in complex systems. Computational simulations are the modern version of the famous *Gedankenexperiment*. *A thought experiment is a device with which one performs an intentional, structured process of intellectual deliberation to speculate, within a specifiable problem domain, about potential consequents/antecedents for a designated antecedent/consequent.* (*Yeates, Lindsay Bertram* 2004, *Thought Experimentation: A Cognitive Approach*). New ideas, proposals, and hypotheses may appear merely speculative; however, they are indispensable to proceed when *in vivo* testing is too complicated, if not impossible: in theoretical biology, computational models are necessary to test the correctness of new proposals. The centrosome was discovered in 1875, it is present in almost all Metazoans, mass spectroscopy has identified as many as 500 proteins [2], nonetheless, after a century and a half, its role remains indeterminate; the idea that only a fraction of the human genome could be functional dates back to the late 1940s: DNA tandem repeats, a relevant part of the genomes (about 50% of the human genome consists of repeats), have been considered nonfunctional sequences, and referred to as *junk DNA*; successively they have been studied and investigated, but their role remains unclear. Computational models check whether new ideas are only mere speculations or can open new per-

spectives.

2. Introduction

More than 400 dog breeds have appeared in just 150 years (the Victorian Explosion), an incredible variety of sizes and shapes, from a Chihuahua to a Great Dane: such a rapid evolution of new shapes challenges the classical theory of evolution. Bilateral symmetry is even more inexplicable: in dog breeds, shapes change, but bilateral symmetry is always respected; to show an example, the average number of nipples in dogs varies from 8 to 10; some dogs may have fewer than 8 or more than 10, depending on genetic factors and breed differences: larger dog breeds tend to have more nipples than smaller ones; in any case, nipples are always bilaterally symmetric. In this explosion of breeds, the role of breeders has been small and marginal: men have always crossed animals suited for work and nutrition, looking for more useful new phenotypes, but only dogs have shown such a wide variety of shapes: dogs are much more variable in size and shape than any other mammal. Breeders search for the best specimens simply by selecting cubs that promise but do not always keep to become better phenotypes and help them to reproduce, however, this is nothing but what natural selection has always done. Behind new phenotypes, there are new genotypes, and the speed of emergence of new genotypes in dogs is surprising. Interestingly, in genes that control morphological variations in dogs, different DNA tandem repeats (TRs) correlate with the rapid morphological evolution of breeds, suggesting a morphogenetic role for satellite DNA: the relevant anatomical differences seen in dogs are associated with differences in satellite DNA [Myers: *Tandem Repeats and Morphological Variation*, [3]. DNA dissimilarity between breeds in dogs is estimated at 27.5% [4], whereas genomic variation in humans is 0.4% (National Institutes of Health, NIH). Fondon and Garner [5] and Sears *et al.* [6] have confirmed that length variations in satellite DNA sequences are a major source of morphological variations: *Repeat expansions or contractions vary in a locus-specific manner and occur at rates up to 100,000 times higher than point mutations because of the distinct mutational mode of slipped-strand. We hypothesize that gene-associated tandem repeats function as facilitators of evolution, providing abundant, robust variation and thus enabling extremely rapid evolution of new forms*. Why are TR mutation rates up to 10,000-fold [7] higher than in other genome regions? The reason is TR DNA remodeling due to the high number of repetitions of identical sequences; TRs have a strong propensity to undergo aberrant recombinations and rearrangements: DNA polymerase slippages, non-disjunctions, recombination, unequal crossing-overs, rolling-circle replications, and multiple jumps of transposable elements (TE) generate different satDNA families [8]-[10]. The large disparity in TRs [11] rather than the small gene diversity between chimpanzees and humans, is associated with the threefold expansion of the human brain and the twofold increase of neuron number in our cerebral cortex [12]: a minimal difference in the genome of *Homo sapiens* relative to Neanderthals, a single-point mutation in the

transketolase-like 1 gene (*TKTL1*), involved in TR methylation [13], is at the origin of the impressive increase of basal radial glial cell divisions, that, in turn, boost the output of upper-layer projection neurons [14]. The correlation between TRs and morphological variations is significant, however, at the current state of the art, it is impossible to demonstrate a direct causal link and confirm that *tandem repeats function as facilitators of evolution*. A computational model [15] suggests that TRs may be iterated to count cell divisions: many TRs are invariable and well-conserved, while others are more variable [16]-[19]; some characters are deterministically reproduced (e.g., the number of teeth, vertebrae, fingers, flight feathers), others are comparatively more variable (gaussian biological variability and interindividual polymorphism). After all, different shapes result from anisotropic growth, *i.e.*, different numbers of cells along prime directions: *If each cell in our arms underwent just one more round of cell division along the proximal-distal axis, we could tie our shoelaces without bending over. How is cell division so tightly regulated?* [20]. Iteration over conserved sequences of TRs is much more accurate than fluctuating morphogen gradients. Dog morphological characters are heritable and transmissible, following Mendel's laws, as pedigrees and cross-breeds show: clearly, growth anisotropy is DNA-coded.

2.1. Centrosome Theoretical Models: Intracellular Trafficking, Cell Cortex Partitioning, and Embryo Divisions

Many animals exhibit mirror-symmetric body plans; however, the cytoskeleton [21] is a chiral structure (from the Greek χείρ, "hand", the most known chiral object): for example, in planarian flatworms, chiral centrioles, dextral and sinistral, are arranged in a bilaterally symmetric pattern across the ventral epidermis [22]: the midline separates the left and right halves, each with only one type of centriole, dextral on the right side, sinistral on the left.

It is convenient to recall some geometrical definitions. On a plane (2D), capital letters such as A, W, Y, and X are intrinsically symmetric: they may be divided into two symmetric halves (mirror images) by a top-bottom line passing through their center of mass; they are called symmetric or bilaterally symmetric.

Not so for letters like E, D, and K, which do not have any intrinsic line or plane of symmetry: on a plane (2D) their mirror images Ǝ, ᗡ and ᴋ cannot be superimposed on the original images without being overturned (overturning occurs in 3D): E, D, and K letters are called asymmetric or chiral, or enantiomorph: asymmetry, chirality, and enantiomorphism are synonyms. Euclidean geometry precludes the construction of a mirror-symmetric structure out of chiral components without the simultaneous use of their mirrored partners: so, pairs consisting of a chiral letter and its mirrored partner, as E Ǝ, D ᗡ, and K ᴋ, better if written as {EƎ}, {Dᗡ}, {Kᴋ} and considered singletons or sets with only one element, are bilaterally symmetric objects, divisible into two symmetric or mirror images, one dextral and one sinistral, by a vertical line passing between the two letters. Pairs such as EƎ, Dᗡ, and Kᴋ are then bilaterally symmetric objects made up of two chiral elements,

each one mirrored partner of the other one. The only difference between paired and unpaired organs is that paired chiral mirror image objects are far from the midline, whereas the two chiral halves of unpaired objects are strictly joined on the midline. Bilateria, the largest group of animals on earth, have unpaired and paired symmetric structures: unpaired bilaterally symmetric organs like the letters A, W, Y, X (cranium, backbone, chest, pelvis, tongue) and pairs of chiral structures as the letters E, D, K (right and left arms and legs). Other organs (heart, liver, spleen) are asymmetric. The distinction between unpaired and paired symmetric structures is more philosophical than physical: the object "Ǝ W ∃" seems made up of two paired, mirror-symmetric, chiral structures (Ǝ and ∃), and one unpaired bilaterally symmetric structure (W); however, "Ǝ W ∃" may be divided by the midline into two chiral, mirror images "Ǝ V" and "V ∃". So, it is better to consider unpaired and paired organs as organs made up of two chiral, dextral and sinistral, halves, mirror images of each other. Euclidean geometry, as said, precludes the construction of a mirror-symmetric structure *out of chiral components*: however, it is possible to realize bilaterally symmetric structures comprised of many not-chiral elements; it is not necessary that in the right and left halves the elements have different shapes, *i.e.*, dextral shape in the right half and sinistral in the left: Lego bricks are *all identical and not chiral*, nonetheless, bilaterally symmetric objects, such as airplanes, may be built. Automata are objects polarized by a chiral tool that gives them the corresponding chiral behavior. Cells are biological automata, externally identical, but intrinsically chiral [23].

Centrosomes are composed of two orthogonal centrioles, called mother and daughter, that are cylindrical organelles comprising nine sets of microtubule triplets; centrosomes are microtubule-organizing centers. They support cytoskeleton, cell division, intracellular trafficking, and ciliogenesis (basal bodies are mother centrioles). During interphase, microtubules are organized in a star-shaped structure (the "aster") that radiates from the unique cell centrosome toward the cell cortex. These geometrical structures suggest the centrosome is the cell 3D geometry organizer [24] [25].

Organisms are not unshaped blobs of cells: cells are orderly arranged, not randomly mixed, as a consequence of oriented cell divisions and precise cortical locations of proteins that control cell and tissue polarity; blastomeres of different phyla control spindle pole positioning to follow different geometric (genetic) programs of division (bilateral, radial, rotational or spiral cleavage); heritable geometric patterns of embryo cleavage are critical developmental steps for proper morphogenesis in all metazoans. Species-specific developmental strategies have emerged and been established: deterministic cleavage patterns with stereotyped division geometries, coded in DNA, are peculiar to each species; the exact positioning of division planes, clearly evident during the first stages of cleavage, is a fundamental process for cell arrangements into embryo anatomical architecture: it defines cell locations and cell-to-cell contacts, with potential immediate impact on lineage specification and morphogenesis.

Heritable cortex partitioning requires astral microtubules labeled by receptors corresponding to their position and orientation: geometric partitioning of the cell cortex is necessary to position polarity proteins and spindle poles (centrosomes) into definite domains; this question is addressed in the program *Iter*.

2.2. About "*in Silico*"

Python is a well-known language, frequently used by researchers and software developers. It is particularly useful for simulating processive cellular functions executed step by step on linear [26]: Python's *for*…*in* and *while* loops perform repetitive tasks, traverse and scan iterable objects like lists and strings, one item at a time; these statements accurately reproduce repetitive biological mechanisms such as replication, transcription, or translation, and closely emulate and imitate their mechanisms; also *if*\|*elif*\|*else*, *break*, *continue*, *and*, *or*, *not*, *pop*() mimic biological functions: they reproduce, *in silico*, biological *in vivo* pathways that may be True or False, e.g., ligand/receptor matching that has or not taken place, or concentration level reaching. All these instructions may be called *biologically compatible*; on the contrary, *classes*, *matrices*, *multidimensional arrays*, *and recursive functions*, which are almost indispensable in programming, are different from biological mechanisms and pathways [27]-[29]. Unlike cellular systems, computers have memory for storing data and organizing stacks (memoization, dynamic programming, overlapping subproblems), necessary for keeping track of recursive calls and their order. In computer science, a stack is an abstract data type that serves as an ordered collection of elements with two main operations: *push* adds an element to the collection, *pop* removes the most recently added element; a procedure is a set of steps based on a set of rules; running a procedure involves following the rules and performing the steps. In other words, iterative functions, used in programming, loop to repeat some part of the code, whereas recursive functions call themselves (rather, recall their code) again and again to repeat it; genetic codes are repeatedly and sequentially executed until "STOP" signals are reached, but neither recall themselves nor organize stacks, queues, and containers to store data: FIFO/LIFO procedures do not have biological corresponding functions. Mandelbrot fractals, Fibonacci's spiral, and the golden ratio are useful to illustrate and simulate biological structures: they are normally (and easily) implemented with recursive functions; golden spirals are logarithmic spirals whose growth factor is φ, the golden ratio (the lowercase form - φ or ϕ - of the Greek letter *phi* symbolizes the golden ratio; sometimes the uppercase form is used for the reciprocal of the golden ratio); many seashells expand in proportion to the golden ratio, whereas the well-known Nautilus shell follows the square root of the golden ratio; biological systems do not deal with square roots: mathematical models reproduce the effects of biological functions but do not simulate their biomechanisms: this is the difference between *biological compatible* statements and *not biological compatible* procedures. Wikipedia proposes a Python program for the golden section search: this implementation does not reuse function evaluations,

exactly as it occurs in biological systems (https://en.wikipedia.org/wiki/Golden-section_search). Iterative biologically compatible functions may implement recursive functions: the program *Recursion vs Iteration* shows that iteration, using only *for…in* instructions, achieves the same results as recursive functions to realize the well-known Koch curve.

The presented programs do not deal with the complexity of the evo-devo processes: rather, they try to replicate only some elementary events that change DNA sequences to generate new complex shapes; the code is intentionally not elegant, but it reproduces faithfully iterative cellular procedures. Therefore, the attached programs *Morphogenesis*, *Iter*, and *Bilateral Symmetry* simulate repetitive biological mechanisms, using only *biologically compatible* statements to propose models that can help to understand and predict how cells behave in different situations.

3. Materials and Methods

Programs

[***For "not-pythonist" readers.***

To run the attached programs, not Python users can follow the simple and clear instructions from Nebraska Lincoln University:

https://cse.unl.edu/~lksoh/Classes/CSCE100_Fall23/install/IDLEInstallation_WindowsSimplified.pdf]

Programs have been developed in Python, version 3.10.8, Windows, 64 bit.

Codes: https://www.researchgate.net/profile/Marco-Regolini/research

The following micro-satellite sequence made of 46 monomers (only partially similar) represents an ordered sequence of centriolar angles (explained in the Discussion) implemented as a list capable of driving the construction of a simple bilateral circular structure (**Figure 1**):

sat_DNA_degree =

['TTTTT', 'ATTAA', 'ATTAG', 'ATTCA', 'ATTCT', 'ATTAA', 'ATTAG', 'ATTAA', 'ATTCT', 'ATTAA', 'ATTTG', 'ATTAA', 'ATTCT', 'ATTAA', 'ATTAG', 'ATTAA', 'ATTCT', 'ATTAA', 'ATTAG', 'ATTAA', 'ATTCT', 'ATTAA', 'ATTAG', 'ATTAA', 'ATTCT', 'ATTAA', 'ATTAG', 'ATTAA', 'ATTCT', 'ATTAA', 'ATTTG', 'ATTAA', 'ATTCT', 'ATTAA', 'ATTTG', 'ATTAA', 'ATTCT', 'AAAAA', 'TTTTT', 'TTTTT', 'ATTAA', 'ATTAG', 'ATTCA', 'ATTCT', 'ATTAA', 'ATTAG']

Each monomer comprises 5 nucleotides with the common initial sequence "ATT" (except for the 0˚).

The last two nucleotides specify an angle: to decode angles (as for amino-acid codons) a redundant correspondence has been utilized, founded on the conserved 40˚ centriolar angle (see Discussion) and the rotational centriolar asymmetry [30] (see Discussion):

```
{
    'TTTTT' : 0,
    'ATTAA' : 40,
```

```
'ATTCC' : 80,
'ATTGG' : 120,
'ATTTT' : 160,
'ATTAC' : 200,
'ATTAT' : 240,
'ATTAG' : 280,
'ATTCT' : 320,
'ATTCG' : 360,
'ATTCA' : 40,
'ATTGA' : 80,
'ATTGT' : 120,
'ATTGC' : 160,
'ATTTA' : 200,
'ATTTC' : 240,
'ATTTG' : 280,
'AAAAA' : 0
}
```

The OUTPUT of this program is a simple bilateral 2D structure (Figure 1 and Figure 2): triangles (red = right, blue = left) represent the "oriented" imaginary disposition of cells on the X-Y plane, simulating the dipodial bifurcation of the embryonic trachea in vertebrates, seen in 2D on a plane orthogonal to the sagittal axis. The Python "turtle" module has realized figures.

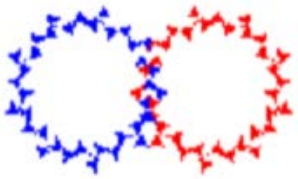

Figure 1. "Bilateral symmetry" program result (see text).

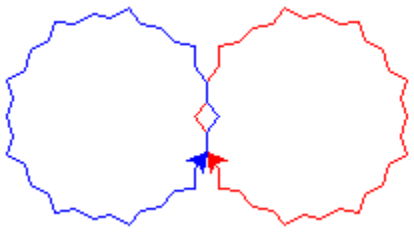

Figure 2. Bilateral symmetry realized by two symmetric devices (Python triangular "turtles").

4. Results

An evolutionary lever to accelerate the genomic capacity of creating novelties

Bilateral Symmetry, *Morphogenesis*, and *Iter* simulate molecular mechanisms, based on TRs, that may function as genomic levers able to accelerate the emer-

gence of complex organs. These codes show a theoretical link between TRs and morphological genomic programs. It is advisable to proceed step by step.

As already said, shapes and sizes result from anisotropic growth, *i.e.*, they depend on the number of cell duplications in prime directions: genetic growth programs control the number of cell divisions and growth directions (as in dog shapes), coordinating determinism and limited degrees of freedom, *i.e.*, gaussian biological variability within fixed limits of variance.

The classical theory of evolution explains well microevolution: bacteria are among the fastest reproducing organisms in the world, doubling every 4 to 20 minutes: millions of new bacteria are generated in one day by a single progenitor; besides this velocity of reproduction, DNA mutation is speeded up through horizontal, *i.e.*, *not* from parent to offspring, DNA exchange mechanisms (transformation, transduction, and conjugation): frequently aided by viruses and phages, these processes mediate massive horizontal DNA transfers, changing genomes immediately, *in loco*, on-site [31]-[33]. Not so in eukaryotes, where the most frequent actors of evolution are single-nucleotide errors in copying DNA, ≈1 per 10^5 nucleotides [34] [35]: single-nucleotide errors act slowly because they do not occur via horizontal DNA transfers, but only through vertical transmission, from parents to offspring; the age of puberty takes days or months, fertility cycles are seasonal or last days, gestation periods takes days or months: therefore a long time elapses between successive generations; in addition, heritable mutations, to be transmitted, must occur only in germinal cells, a quite small percentage of the whole number of cells, reducing the likelihood of the emergence of more successful genotypes. Single-celled, asexually reproducing, organism populations have numerical orders of magnitude not comparable to populations of multicellular, sexually reproducing, organisms; the complexity and length of DNA programs for assembling cells in tissues and organs are not equivalent to single-celled brief codes. Hence, single-nucleotide errors do not seem fast enough to be compatible with the appearance of the sophisticated architectures of complex organs. The rapid evolution of the cerebellar [36] and the cerebral cortices and non-cortical areas [37] in great apes and, overall, in humans, poses many questions about the explosion of large changes in cell number, morphology, and composition: cell density arrangements and connectivity, horizontal layers or laminae, and vertical radial columns or modules have emerged contemporaneously in every part of the brain. Some accelerators of evolution must exist in eukaryotes. TR mutation rates [38] are much higher (from 10^{-6} to 10^{-2} nucleotides per generation) than mutations in coding DNA sequences (≈10^{-9} nucleotides per generation). Many studies have investigated the possible role played by TRs and TEs, also known as jumping genes (see: Gemayel *et al. Variable tandem repeats as facilitators of the rapid evolution of regulatory and coding sequences* [39], Mert *et al. Evolution of tandem repeats is mirroring post-polyploid cladogenesis in Heliophila* [40]). The self-remodeling propensity of satDNA may bridge the gap between microevolution and macroevolution timing [41]-[43]: massive TR expansions and contractions in coding regions are a major source of phenotypic variations [13]; alterations of the number of TRs inside coding regions [44] [45]

are associated with differences in limb and skull morphology in canine breeds [46] [47] suggesting the hypothesis that TRs are iterated for counting cell divisions [15] and regulating gene expression and transcription.

Thus, that is the question: Are DNA codes like computer programming codes? Do DNA and machines share the same logic? DNA programming is based on Boolean algebra and exhibits algorithms like those observed in machine languages [48], and common algorithms, Mandelbrot fractals, for example, efficiently simulate complex morphologies; however, attention is required. Fractals or Fibonacci sequences are normally implemented through recursive functions, which work quite differently from biological processes: cells ignore stacks and queues, containers to store data, and FIFO/LIFO procedures. On the contrary, iterations (*for*…*in* and *while* cycles) faithfully reproduce DNA processive pathways: the *iteration protocol* works, step by step, on linear sequences, just like many biological molecular mechanisms work step by step on linear nucleotide sequences (DNA duplication, transcription, translation, polymerization of biomolecules, etc.). Iteration, using only repeated *for*…*in* instructions, reaches the same results as recursive functions. Given that fractals reproduce accurately developmental mechanisms of growth and may be implemented by biologically compatible iterative loops, the answer to the previous question is: Yes, it seems possible that machine and DNA codes share the same logic. Thus, the introduced programs, simulating repetitive biological mechanisms through elementary and *biologically compatible* iterative procedures, show that TRs, if iterated to count cell divisions, can accelerate the emergence of new shapes and sizes, taking advantage of their propensity to massive mutations and following the iteration protocol of machine algorithms.

The program *Morphogenesis* demonstrates that just a single-bit-error can act as a powerful lever that dramatically changes the output: the only requirement is that it occurs in strategic positions. A single-bit-error changes the instruction for calling the recursive function *koch*: a 6 in place of a 2, *i.e.*, *koch*(*l*, *r*, ***6***, *5*) *instead* of *koch*(*l*, *r*, ***2***, *5*).

[To illustrate that this is a minimum error, it is convenient to recall that the extended ASCII table (American Standard Code for Information Interchange) is based on the Windows-1252 character set, probably the most widely used 8-bit character encoding system in the world: ASCII is an 8-bit table with 256 characters and symbols. Bits are stored in memory using capacitors that hold electrical charges: the charge determines the state of each bit, high or low, which, in turn, determines the bit's value, 1 or 0. The number 2, in the ASCII 8-bit (or 1-byte) set, is assigned a decimal value of 50, which is equivalent to the 8-bit binary value of 0011 0010. In contrast, the number 6 is assigned a decimal value of 54, which is equivalent to the 8-bit binary value of 0011 0110].

A **6** in place of a **2**, as the third parameter in the call of the function, is just the consequence of the following minimum change: a **0** instead of a **1** in the 6th bit (reading from left to right) of the byte of their binary codes (0011 0***1***10 vs 0011 0***0***10); this is the least possible error, really a single-bit-error that simulates a sin-

gle-nucleotide-error. It is very important to underline that this error has occurred, as said, in a strategic position, where is the checkpoint for controlling the number of repeats. If a similar error had occurred in the letter "c" of "koch", it would have changed "koch" into to "koah": the machine would not have understood such a statement and the execution of the program would have broken down; 0110 00**1**1 is the binary code for the letter "c", and 0110 00**0**1 is the code for the letter "a": the same error, a **0** instead of a **1**, changes the instruction *koch*(*l*, *r*, ***6***, *5*) into an unintelligible *koah*(*l*, *r*, ***6***, *5*).

So, the instruction *koch*(*l*, *r*, ***6***, *5*) *instead* of *koch*(*l*, *r*, ***2***, *5*) generates an impressive variation of shape in an imaginative structure (**Figure 3** and **Figure 4**); notably, bilateral symmetry is respected and conserved. It is possible to imagine that a similar error, a casual slippage that duplicates a long TR sequence, causes a similar enormous change of shape: as seen, TR massive expansions and contractions in coding regions are a main source of phenotypic variations [13] [44] [45].

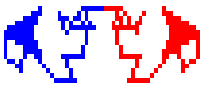

Figure 3. Graphic of the function "*koch*" called with "*koch*(*l*, *r*, ***2***, *5*)".

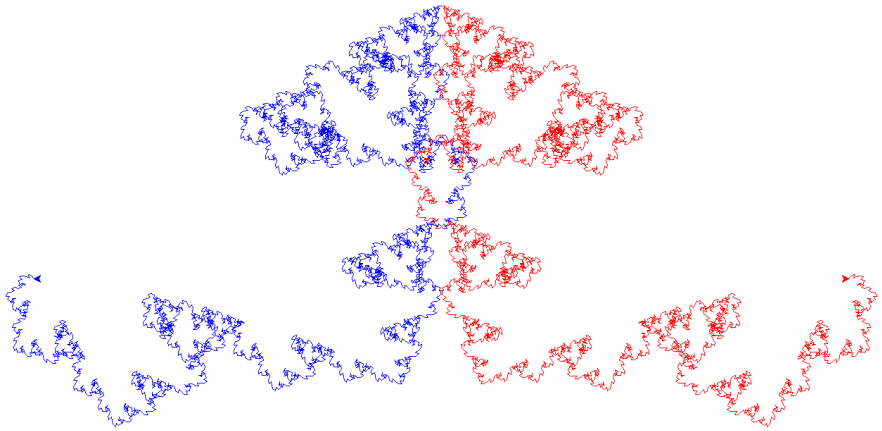

Figure 4. Graphic of the function "*koch*" called with "*koch*(*l*, *r*, ***6***, *5*)"; *koch*(*l*, *r*, ***6***, *5*) instead of *koch*(*l*, *r*, ***2***, *5*) generates an impressive variation of shape. Note that the difference between the codes of "6" and "2" consists in only one bit ("**0**" instead of "**1**") in the 6th bit of the byte of their binary codes: 0011 0**1**10 vs 0011 0**0**10.

The small structure in **Figure 3** could be a butterfly wing pigmentation pattern or a minimal neuronal arrangement; from this small structure, present in the previous generation, a completely different big structure occurs in the offspring through a single mutation in TRs inside coding regions (**Figure 4**): a large expansion of the wing pattern ground plan or an explosion of cortical neuronal arrangements and connectivity; eventually, subsequent evolutionary transformations can obtain new goals by taking advantage of these new structures.

Thus, a simple, trivial single-point-mutation, a **0** instead of a **1** in the binary

code, acts as a powerful coding lever, capable of realizing large phenotypic changes: this simulates a small (and then likely) genomic variation occurring in some, prone to duplicate, TR sequence…but…only if cells were able to execute recursive functions: unfortunately, they are not. Nonetheless, using iterative *biologically compatible* functions it is possible to mimic DNA transpositions, achieving similar results: the program *Recursion vs Iteration* shows how annealed transpositions of *for...in* cycles, that are *biologically compatible* iterative instructions, reproduce the same curve designed by not *biologically compatible* recursive functions (**Figure 5**). Fractals and Fibonacci sequences, normally implemented through recursive functions, are fascinating: they describe many biological geometries as in pineapple, sunflower, cabbage, and phyllotaxis, inexplicable by Turing's *Chemical Basis of Morphogenesis* (a reaction-diffusion theory of morphogenesis). Multiple repetitions of *for…in* cycles can substitute recurrences. The structure of the introduced code reproduces credible successive evolutionary events: DNA duplications, easy and frequent in satDNA [49], inversions, partial deletions, expansions of short and long sequences of satDNA, and repetitive transposition due to TEs [50] [51].

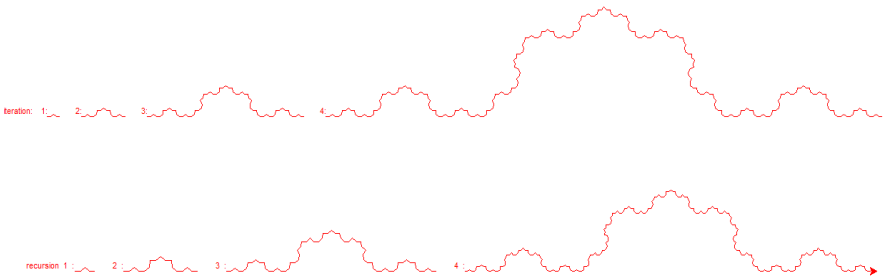

Figure 5. Recursion and iteration realize similar structures.

The paradigm of the code of *Recursion vs Iteration* (**Figure 6**) is a persuasive simulation of well-known DNA molecular mechanisms: V(D)J recombination occurring in developing somatic cells, evolutionary duplication of Hox genes, and *α* satellites within human centromeres (**Figure 7**, **Figure 8**) where they form blocks of satellites, called higher order repeats (HOR).

Code iterations with *for...in* cycles (**Figure 6**) are surprisingly faithful and accurate in imitating the evolutionary process of HOR organization as images from Aldrup-MacDonald, McNulty, and Sullivan show (**Figure 7**, **Figure 8**):

- uppercase "**X**" is a block consisting of three lines of code:

```
for angle in [40, −80, 40, 0]:
    r.forward(5)
    r.left(angle) "
```

- lowercase "**x**" is a block consisting of these two lines of code:

```
for angle in [40, −80, 40]:
    r.left(angle) "
```

```
""" iteration order 1 """     # (1)
r.write("iteration:  1", font=("Arial", 12, "normal"))
r.penup()
r.forward(80)
r.pendown()
for angle in [40, -80, 40, 0]:          # THIS
        r.forward(5)                    # IS
        r.left(angle)                   # THE CODE '1
"""iteration order 2"""                 # 2 = (1)_(1)
r.penup()
r.forward(15)
r.pendown()
r.write(' 2 ', font=("Arial", 12, "normal"))
r.penup()
r.forward(20)
r.pendown()
for angle in [40, -80, 40, 0]:                  # REPETITION
    r.forward(5)                                #  OF
    r.left(angle)                               #  CODE '1'
for angle in [40, -80, 40]:                     # [partial duplication
    r.left(angle)                               #  of code 1
    for angle in [40, -80, 40, 0]:              # REPETITION
      r.forward(5)                              #  OF
      r.left(angle)                             #  CODE '1'
"""iteration order 3"""                 # 3 = (2)_(2) = [(1)_(1)]_[(1)_(1)]
r.penup()
r.forward(15)
r.pendown()
r.write(' 3 ', font=("Arial", 12, "normal"))
r.penup()
r.forward(20)
r.pendown()
for angle in [40, -80, 40, 0]:                  # REPETITION
    r.forward(5)                                #  OF
    r.left(angle)                               #  CODE '1' . . . . . .
```

Figure 6. Code from "Recursion_vs_Iteration".

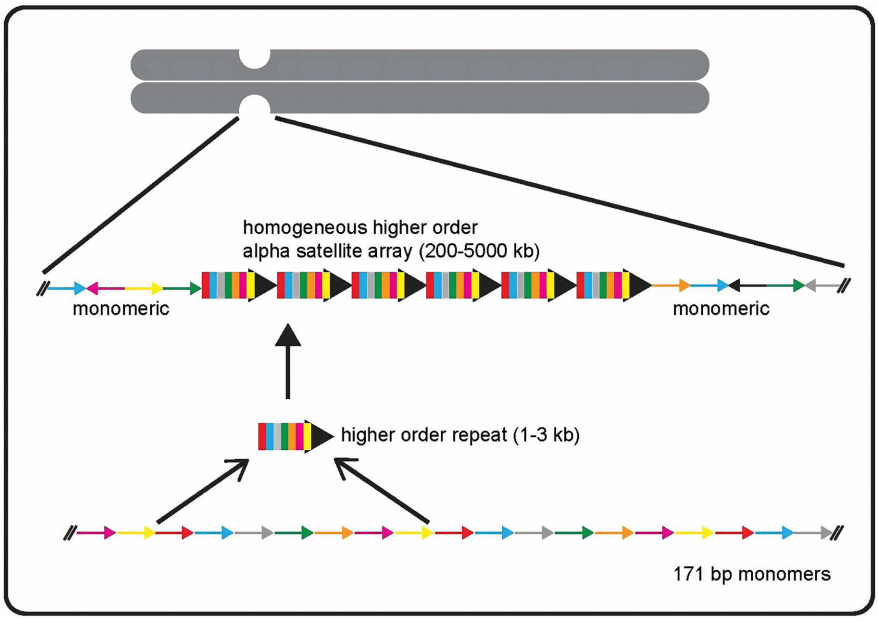

Figure 7. The genomic organization of human centromeres. The primary sequence at human centromeres is alpha satellite DNA that is based on 171 bp monomers (colored arrows) organized in a tandem head-to tail fashion. The monomeric sequences differ by as much as 40%. A set number of monomers give rise to a higher order repeat (colored bars with black arrowhead) and confer chromosome-specificity. Higher order repeats are themselves reiterated hundreds to thousands of times, so that the alpha satellite arrays are highly homogenous and span several hundred kilobases to several megabases. Unordered monomeric alpha satellite DNA flanks the higher order arrays, becoming progressively more divergent farther away from centromeric core. [From: Aldrup-MacDonald E M, Sullivan, B A (2014). The Past, Present, and Future of Human Centromere Genomics. Genes, 5(1), 33-50. https://doi.org/10.3390/genes5010033 under the terms and conditions of the Creative Commons Attribution license (http://creativecommons.org/licenses/by/3.0/). Open access: Creative Commons CC BY 4.0 license.]

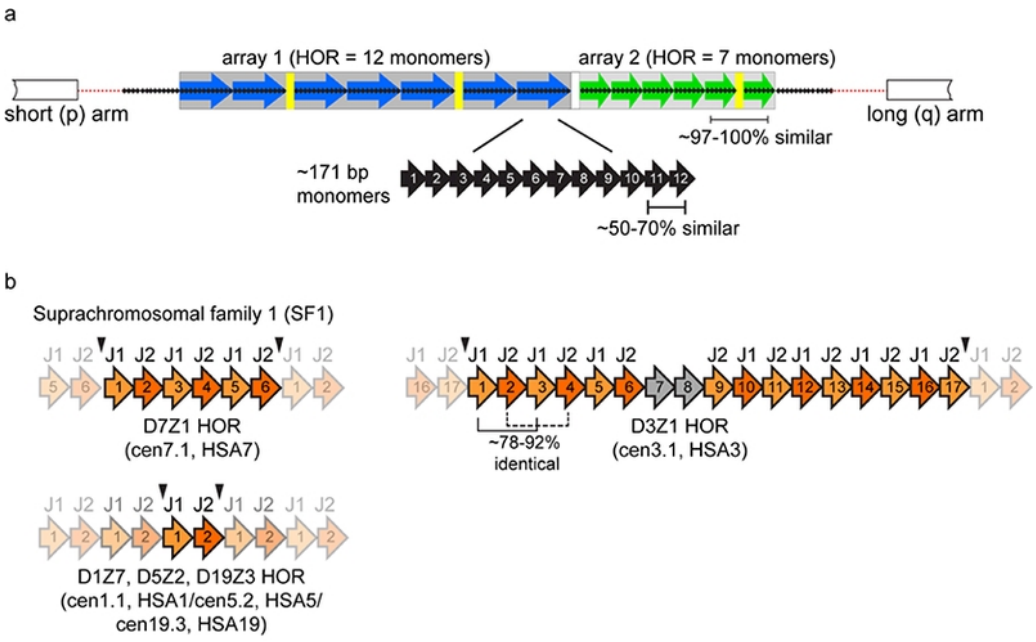

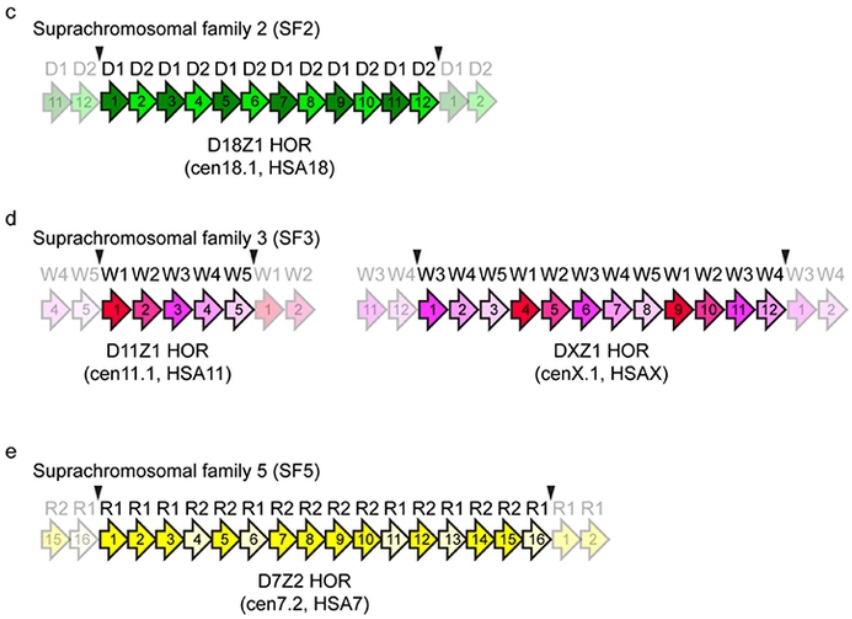

Figure 8. Array and chromosome-specific organization of alpha satellite DNA. (a) Schematic of the general organization of alpha satellite DNA arrays at human centromere regions. Human chromosomes can have either one or more distinct higher-order repeat (HOR) arrays. HORs are array- and chromosome-specific. A defined number of individual monomers (black arrows) that are 50% - 70% identical in sequence are arranged tandemly to form a HOR unit; shown here as either a 12 monomer HOR (blue array) or 7 monomer HOR (green array). Monomers are numbered by their position within the HOR and not based on their homology between two distinct HORs. The HORs are repeated hundreds to thousands of times to create homogenous arrays in which HOR within a given array are 97% - 100% identical. The HOR array is flanked by degenerate alpha satellite DNA monomers (small black arrays) that lack hierarchical structure and separate the HOR array from the chromosome arrays. HOR arrays are interrupted by other repetitive elements, such as transposable elements (TEs, yellow) but the extent of TE distribution across arrays is unclear due the lack of linear, contiguous assemblies of endogenous alpha satellite arrays. (b) Alpha satellite HOR arrays have been classified into suprachromosomal families (SF) that are related based on monomer type and organization. SF1 arrays are organized as alternating dimers of J1 and J2 monomers (D7Z1, cen7.1), although variation in the regular organization of monomers occurs on some chromosomes, like the D3Z1 (cen3.1) array of Homo sapiens chromosome 3 (HSA3). Additionally, the HORs can be shared among chromosomes, such as the D1Z7 (cen1.1) array that is also present as D5Z2 (cen5.2) on human chromosome 5 (HSA5) and D19Z3 (cen19.3) on HSA19. Each array-specific HOR unit is operationally defined by restriction enzyme sites (black arrowheads) that demarcate the last monomer of one HOR unit and the first monomers of the next HOR unit. Opaque shading illustrates the linear, reiterated nature of HOR units. (c) SF2 is composed of a different dimeric structure based on D1 and D2 monomers. D18Z1 (cen18.1) on HSA18 has SF2 organization. (d) SF3 is based on a pentameric organization of monomers W1-W5. D11Z1 (cen11.1) is an example of a perfect pentameric HOR unit, while DXZ1 has an irregular organization of W1 - W5 monomers. (e) SF5 arrays are defined by R1 and R2 monomers, although they largely lack the dimeric organization observed for SF1 and SF2 arrays. Some arrays have HOR unit structure, such as the D7Z2 (cen7.2) array of HSA7. D_chromosome_Z_number is the original Human Genome Project locus definition of alpha satellite arrays. The newer UCSC Genome Browser annotations of distinct HOR arrays (cen_chromosome number.array number) are also included. [From: McNulty SM, Sullivan BA. Alpha satellite DNA biology: finding function in the recesses of the genome. Chromosome Res. 2018 Sep; 26(3): 115-138. SPRINGER NATURE LICENSE Number 5921370713854 Dec 03, 2024]

The "***x***" code derives from "**X**" by two little deletions, a common and recurrent evolutionary event:

```
for angle in [40, −80, 40, 0]: # '0' has been deleted
    r.forward(5)    # 'r.forward(5) 'has been deleted
    r.left(angle)
```

Here is the structure of successive duplication-transposition and joining: 1, 2, 3, 4 are the consecutive stages of duplication and transposition (attention to brackets):

1: $\underline{\mathbf{X}}$ → 2: $(\underline{\mathbf{X}}_{\mathbf{x}}\underline{\mathbf{X}})$ → 3: $[(\underline{\mathbf{X}}_{\mathbf{x}}\underline{\mathbf{X}})_{\mathbf{x}}(\underline{\mathbf{X}}_{\mathbf{x}}\underline{\mathbf{X}})]$ → 4; $\{[(\underline{\mathbf{X}}_{\mathbf{x}}\underline{\mathbf{X}})_{\mathbf{x}}(\underline{\mathbf{X}}_{\mathbf{x}}\underline{\mathbf{X}})]_{\mathbf{x}}[(\underline{\mathbf{X}}_{\mathbf{x}}\underline{\mathbf{X}})_{\mathbf{x}}(\underline{\mathbf{X}}_{\mathbf{x}}\underline{\mathbf{X}})]\}$

Each step consists of a duplication-transposition of the previous stage, then joined by "$_{\mathbf{x}}$":

$2 = (1_{\mathbf{x}}1)$; $3 = [2_{\mathbf{x}}2]$; $4 = \{3_{\mathbf{x}}3\}$;

stage 2 ($\mathbf{X}_{\mathbf{x}}\mathbf{X}$) consists of the duplication of the sequence "**X**" of stage 1, joined each other by the short sequence "$_{\mathbf{x}}$" (derived from **X** by two little deletions); similarly, stage 3 $[(\mathbf{X}_{\mathbf{x}}\mathbf{X})_{\mathbf{x}}(\mathbf{X}_{\mathbf{x}}\mathbf{X})]$ consists of the duplication of the sequence ("$\mathbf{X}_{\mathbf{x}}\mathbf{X}$") of stage 2 joined in turn by the short sequence "$_{\mathbf{x}}$".

The list *[40, −80, 40, 0]* simulates a short TR sequence whose nonidentical monomers carry angle information (see further).

During evolution, many DNA sequences have been converted by TEs into TRs [50] or translocated into a gene. Repetitive elements can be remodeled into repetitive noncoding or coding sequences [45]. Casual massive cluster duplications, inversions, and transpositions of satDNA sequences [52] are evolutionary mechanisms able to approach fractals, and generate fast and large variations of shape, eventually subjected to natural selection. *Morphogenesis* and *Recursion vs Iteration* show a method to simulate such an important genetic lever suggesting that TRs can accelerate and sustain the evolution of complex organs.

4.1. Bilateral Symmetry

The emergence of bilateral symmetry during evolution, probably 600 million years ago, provided many advantages in locomotion. How did it emerge? Is it possible that bilateral symmetry emerged once and for all in the ancestor of Bilateria?

Bilateral symmetry is simple, (no matter 2D or 3D), *x* coordinates change their sign: they must be multiplied by −1, absolute values remain unchanged, signs change; a point A (*x*, *y*, *z*) is symmetric to its mirror image A' (−*x*, *y*, *z*) relative to the sagittal *yz* plane. To transform Lego bricks or cells into automata, each one must be polarized and equipped with a chiral tool, dextral "**Γ**" in the right half, sinistral "**⅂**" in the left half: such a chiral tool allows each automaton to execute the same topological instructions in dextral/sinistral modalities, and know its position and orientation in the general reference system of the whole organism.

To better explain this concept, the following thought experiment is useful: in an elementary compass, on its baseplate, a wind rose ring is depicted, showing North and South positioned on the vertical *y-axis*, and West and East on the horizontal *x-axis*; multiplying the *x* coordinates by −1, they change from positive to negative, so, West and East are flipped and a new symmetric compass is realized:

it is the mirror image of the original, then, bilaterally symmetric to it (Figure 9). Two individuals, one equipped with a conventional compass and the other with a mirror image of the original compass in which East and West marks appear swapped, carrying out the same geographic instructions, travel along two symmetrical pathways (Figure 9). The difference is inside the tools, not in the coded instructions. This is a fast and simple evolutionary strategy, likely and able to explain the emergence of bilateral symmetry once and for all in the ancestor of Bilateria. What about its molecular basis?

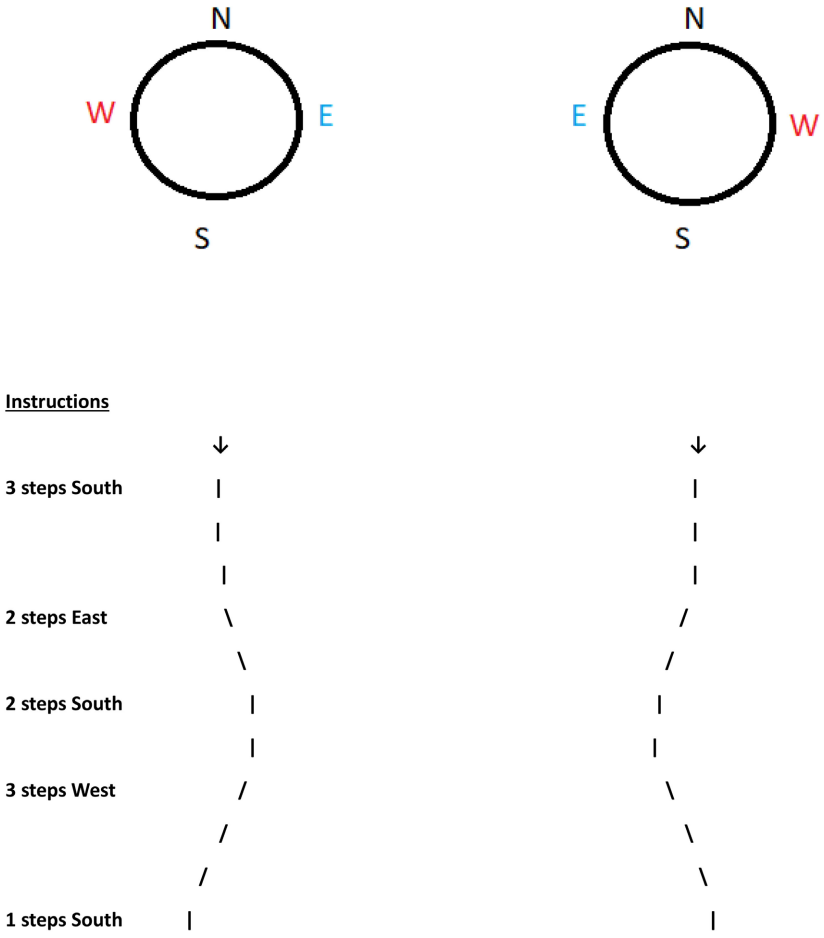

Figure 9. Two symmetrical compasses ("executors") have been prepared; carrying out the same pattern of geographic instructions, they will drive to travel along two symmetrical paths: the difference is inside the "executors", not in the code instructions.

An increasing number of researchers have investigated centrioles' ultrastructural and molecular architecture, confirming that centrioles are chiral structures and showing how bilaterally symmetrical patterns can emerge from chiral cellular cytoskeletons [22] [23] [53]-[59]. Again, it is convenient to proceed step by step. Live images [22] show inherently asymmetric centriole networks, organized in the planarian epidermis by ODF2 and VFL1/3 proteins (centriolar components), independently of planar polarity cues: this is evident at the midline and the posterior

end, where polarity cues have a limited effect; centrioles/basal-bodies appear arranged in a bilaterally symmetric pattern across the ventral epidermis, and this pattern is generated by centrioles with prominent chiral asymmetric properties (rotational polarity of basal feet and rootlets).

In the zebrafish laterality organ, the Kupffer's vesicle, Ferreira *et al.* [54] measured motile and immotile cilia orientation, relative to the midline, discovering that in the left and right side of the early vesicle (3 somite stage) primary cilia orientation is markedly mirror symmetric: *While right-sided cilia are almost perfectly oriented along the meridional direction* (*+1˚*), *cilia in the left hemisphere exhibit a strong tilt following the flow direction* (*=+28˚*); later (9 - 14 somite stages) cilia orientation rotates 20˚ toward the right, showing a dextral orientation over the whole vesicle, yet maintaining a similar angular difference of ≈30˚ between the left and right side. *These results show that cilia orientation is asymmetric in the Kupffer's vesicle and follows a dextral chirality*. Hence, primary cilia (and their centriole/basal bodies) possess a real chiral structure [30]. Woglar *et al.* [59] demonstrated a cryptic chirality underneath the mirror symmetry of centrioles in planarians (bilaterally symmetric organisms). These results provide insights into how animals can build tissues and organs with bilaterally symmetric patterns from chiral cellular constituents, suggesting that centriolar microtubule triplets on the left and right side possess specific characteristics.

In this paper, this question has been studied through computational simulations to ascertain the role that, in the left and right halves of the whole organism, left and right centrosomal enantiomeric mother centrioles play in driving the formation of 3D bilaterally symmetric structures during evolution and development.

4.2. Bilateral Symmetry and Zygote Centrioles

Centriole transmission is not a trivial, irrelevant function: oocytes, including mammals, lack centrioles, so, the zygote inherits only the sperm centriole: eventually, it provides four centrioles, two for each centrosome because two centrosomes are necessary for the mitotic spindle: centrosomes possess two orthogonal centrioles, the inherited *mother* centriole, and a newly formed *daughter* centriole: each new centriole (called *daughter*) is formed by duplicating the pre-existing *mother* centriole, which acts as a platform, not as a template, for the new nascent centriole. Because the zygote inherits only one functional centriole, the origin of the second interphase centriole is unclear [60]. In insects, the sperm possess a second atypical centriolar structure [61]: is it the kernel for building a mirror-symmetric centriole? Do vertebrates also possess a similar atypical structure that may be the origin of a mirror-symmetric centriole? Is it involved in left-right bilateral symmetry? Is this atypical centriolar structure assembled as a mirror image of the paternal centriole?

Genes and DNA are identical in each cell of the same organism; bilaterally symmetric structures are realized as left-handed (sinistral) or right-handed (dextral) depending on the side from which the cells derive, *i.e.*, whether they derive from

dextral or sinistral precursors; cells behave as automata that know their orientation toward the sagittal plane of the whole organism; mother centrioles, because of their particular and unique mechanism of duplication, transmit to daughter cells an oriented (common and shared) left- or right-handed, reference system, suggesting that centrioles are chiral tools, dextral and sinistral, bilaterally symmetric, capable of driving cells to adopt dextral or sinistral behavior and realize chiral, bilaterally symmetric structures. Do the first two blastomeres possess two symmetric tools (centrosomes) that allow them to build two symmetric structures, left-handed in the left body half and right-handed in the right half, following the same genetic instructions? Are the two first blastomeres already patterned as left and right? In other words, are they the founder cells that state the left/right fate of their progeny, *i.e.*, are they the progenitors of the two symmetric halves of the organism?

Some authors [22] suspect that centriole chirality, *i.e.*, dextral and sinistral centrioles, acts downstream or in parallel to planar polarity cues. In planarians, the midline separates the left and right halves, each one with only one type of centriole, dextral on the right side and sinistral on the left: basal feet and rootlets appear chiral asymmetric in electron microscopic views [22].

In vertebrates, asymmetric organs, such as the heart, normally are built in a fashion known as *situs solitus*, but other anatomical topographies are well known: *situs inversus*, transmitted both as a recessive autosomal and X-linked character, *situs specularis* evidenced in monozygotic twins; these anatomical topics confirm that in germ cells and zygotes, the sets of genes responsible for the chiral assembling of centrioles are attentively controlled (silenced or triggered).

As seen, if one person uses a conventional compass and another person, through an elementary small change (multiplying x coordinates by −1), swaps East and West, these two symmetric, chiral, or enantiomorph, compasses translate the same code of geometric instructions into two symmetrical paths (**Figure 9**); the difference is inside the tools, not in the code, and this, evolutionary speaking, is quite likely, because it requires a unique trivial occurrence, once and for all, in a common ancestor. Similarly, in the programs *Morphogenesis* and *Iter* (**Figures 3-5**) only one byte of code, a *minus* sign, "−", produces two enantiomorph tools that, in turn, follow a unique program to realize left and right graphics.

Below is a schematic representation of zygote centriole assembling to better resume and explain the previously cited findings:

i) inherited sperm centriole (dextral chirality is supposed): **Γ;** top view:  ;

ii) first step: assembly of a new centriole backbone **I**;

iii) second step: centriole backbone decoration with opposite chirality: **Ɪ;** top view: .

4.3. Bilateral Symmetry and Centrosomes

The program *Iter* tests the capability of TRs to build bilaterally symmetric structures, taking advantage of centrosomes. Centrosomes are made up of two orthog-

onal centrioles, each one consisting of nine sets of short microtubule triplets, arranged in a cylinder; rotational asymmetry and non-equivalence of centriolar triplets (as the rotational asymmetry and non-equivalence of the marks in the compasses used in the previous thought experiment) have been conserved from ciliates to humans [30]: the nine triplets are different from each other because each one is labeled by its unique, peculiar, individual, distinctive molecular receptor. Enantiomorphism of centrioles (such as the rotational symmetry of the two compasses above described) may easily sustain bilateral symmetry: a simple error (mutation + duplication) in the code for centriole generation originates two rotationally symmetric centrioles [62], giving to descendants the code for two symmetric tools, capable of managing bilateral symmetry in any structure (**Figure 10**, **Figure 11**). The program *Iter* simulates the dipodial bifurcation of the embryonic trachea, seen in 2D on a plane orthogonal to the sagittal axis (**Figure 1**); the instruction *stamp* simulates the division of a cell: the mother cell remains in its actual position, and its daughter is generated in a coded direction, maintaining the memory of previous steps: its actual orientation is simply the vectorial sum of

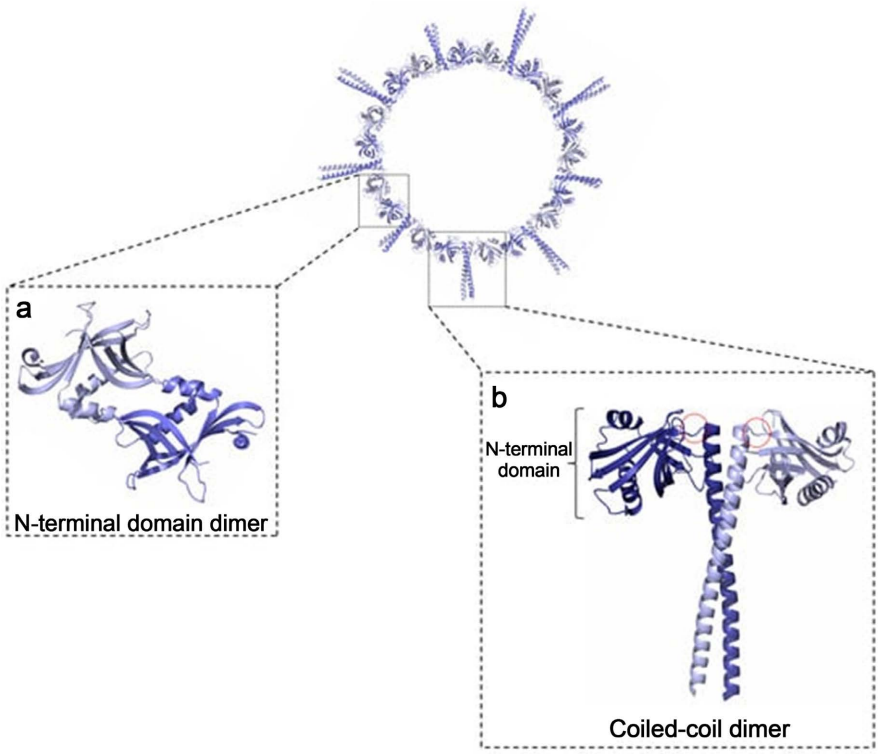

Figure 10. SAS-6 oligomerisation. A SAS-6 ring containing nine protein dimers is shown. SAS-6 self-assembles into rings via two dimerisation interfaces mediated by (a) an N-terminal globular domain (NN) and (b) a coiled coil (CC) 35 to 50 nm long, depending on species. The full extent of the SAS-6 coiled coil and a disordered C-terminal protein region are not shown. Hinge regions connecting the SAS-6 N-terminal domains with the coiled coil are indicated by red circles in (b). [Ford JE *et al.* Coupling Form and Function: How the Oligomerisation Symmetry of the SAS-6 Protein Contributes to the Architecture of Centriole Organelles. Symmetry. 2017; 9(5):74.]

1. =Ǝ---8---ϕ---H---θ---I---Θ---Φ---X---O

2. = 8---ϕ---H---θ---I---Θ---Φ---X---O---E

3. =Ǝ---O---X---Φ---Θ---I---θ---H---ϕ---8

Figure 11. = socket; Ǝ--- plug (the beginning of the sequence); O---X---Φ---Θ---I---θ---H---φ---T sequence of 9 receptors; if overturned (reversed) nothing changes. 1: original sequence; 2: plug transposition; 3: when the transposed plug enters the socket, the receptor sorting is flipped (swapped).

precedent changes of direction. In the code, each cell is polarized and equipped with a chiral tool, a simple +/− sign (in the code the + sign has been omitted, as usual in math); dextral and sinistral cells, respectively in the right or left halves, know their intrinsic reference system (front, rear, left, right) and their position and orientation in the general reference system of the whole organism. The program does not follow the simultaneous development of the bud for the left and right bronchus: it shows in two subsequent steps how mesenchymal cells divide and arrange themselves to build first a right structure and then the left one, to underline that the same code is executed in two different modalities, by chiral right- and left-handed, bilaterally symmetric, enantiomorph tools: the only difference in the code is a minus sign, "−":

"*x = decode[satRNA.pop(0)]*" vs "*x = - decode[satRNA.pop(0)]*".

The ASCII byte for the "+" sign is 0010 1**01**1 whereas the "−" sign code is 0010 1**10**1: a simple inversion of the penultimate two bits. Similarly, a single mutation (**Figure 11**) has originated two rotationally symmetric tools; this is quite easy, simple, and credible. It is an evolutionary *una tantum* (once and for all) event, occurred in an ancestor, giving the capability of executing an infinity of different codes (for different structures) in symmetric, dextral and sinistral, modalities.

4.4. Bilateral Symmetry and TRs

To plan anisotropic growth, the number of cells is responsible for size, while different shapes depend on different tilting (angles) of growth directions.

In the programs *Iter* and *Bilateral Symmetry* the sequence *sat_DNA_count* is an iterable TR sequence of monomers, used to count cell divisions, taking track of each step by progressive epigenetic methylations of succeeding monomers (see Regolini: *DNA Tandem Repeats as Iterable Objects to Count Cell Divisions*: *A Computational Model* [15]). The *in silico* micro-satellite "*sat_DNA_degree*" is an iterable sequence of TR monomers, each one responsible for the orientation of the division plane, *i.e.* the geometrical positioning of spindle axes and poles: each monomer consists of five nucleotides, the first three are a consensus sequence

(ACT), the last two are the code for a multiple (**Figure 10**) of the centriolar 40˚ angle (40˚, 80˚, 120˚…); similarly as codes for amino-acids, the redundancy of the code for 9 angles (360˚/40˚ = 9; dispositions with repetitions of k objects out of n is n^k, then 2 nucleotides out of 4 is $4^2 = 16$, more than 9) has been taken into account. In this program, the nine, non-equivalent, centriolar triplets are labeled by nine different receptors ("*sat_RNA*") corresponding to the above angle codes (such as codon-anticodon correspondence). The 2nd cytosine of each monomer in "*sat_DNA_degree*" is expected to be progressively methylated at each division cycle to silence the monomer and take account of the steps already made [15]; *sat_DNA_degree* is the code for building a particular structure: structures are planned by their own sequence of angles (the interplay between oriented cell divisions and planar polarity cues is beyond the purpose of this article [63]); the sequence *sat_DNA_degree* is read step by step. *i.e.*, division after division, once per cell division, translated one monomer at a time into a *sat_RNA* (*sat_RNA.pop*(*0*)) that is sent to the mitotic machinery to orient spindle poles and axis; finally, information is transferred to the variable *x*, like a tRNA, that matches with the corresponding centriolar triplet on the centrosome (see Discussion); this way, genetically coded geometric projects are executed to build every organ.

In the program *Morphogenesis*, bilateral symmetry is realized by the same code for both the left and the right sides, with only one line that prepares two symmetric tools, two Python Turtles (named "r" = right and "l" = left); the difference consists of only one byte of code, a *minus* sign (*r.left*(*−90*) vs *l.left*(*90*): the chiral right-handed tool turns **−90˚** leftward, whereas the chiral left-handed tool turns **+90˚** leftward.

4.5. A Second Evolutionary Lever to Accelerate the Genomic Capacity of Creating Novelties

Organisms, as said, are not unshaped blobs of cells: anisotropic growth is the consequence of growth in prime directions. Iterable sequences of TR monomers responsible for both the size (*sat_DNA_count*) and the orientation of the division plane (*sat_DNA_degree*): they are subject to DNA changes, as is common in TRs, DNA polymerase slippages, non-disjunctions, recombinations, unequal crossing-overs, rolling-circle replications, and multiple jumps of TE generate new TR sequences; the order of monomers in a sequence is then remodeled and rearranged, causing the emergence of new shapes. Because of the described capability of managing both the number of cell divisions and the direction of growth, TRs may be really responsible for the rapid emergence of new phenotypes, as those described in dog breeds.

5. Discussion

Different works show a correlation between TRs and anatomical variations in dog breeds; other studies have found a cryptic chirality underneath the mirror symmetry of metazoan tissues. The programs introduced here have tested whether

and how TRs and centrosomes can execute these tasks.

5.1. Emergence of Complex Organs

Different shapes, as in dog breeds, ultimately, are the consequence of DNA-coded anisotropic growths: different arrangements of cells mean different numbers of cell divisions along special directions. Computer models help to shed light on this argument. A computational model [15] suggests that TRs may be Iterated to count cell divisions. Many TRs are highly conserved while other sequences are more variable [17]-[19]: taking advantage of this genetic characteristic, TRs may manage the determinism seen in particular stages of development and supervise the intra- and inter-individual variability observable in different stages, which supports morphological controlled (*i.e.*, not anarchist and disordered) biodiversity; fiddler crabs provide an example of planned different numbers of cell divisions along special directions: they are sexually dimorphic, females have two small claws and no visible asymmetry, whereas males have a single minor claw, with which they feed, and a hypertrophied, well-shaped, major claw. The correlation between TR variability and the evolution of shapes is based on solid foundations: the propensity of TRs to undergo frequent evolutionary recombinations and rearrangements, although, at the state of the art, it is not possible to demonstrate a direct causal link between TRs and morphological variations. However, several studies on the butterfly wing pattern ground plan [64]-[67] have shown that deeply ancestral, multifunctional noncoding elements underlie rapidly evolving trait systems: conserved TRs and TEs, often interspersed inside genes or regulatory regions, are involved in pigment synthesis, and are responsible for wing pattern variations. This mechanism has been simulated in *Recursion vs Iteration* and *Morphogenesis* which draw curves (**Figure 5**), per se insignificant, but interesting for the code that reproduces the outcomes of massive duplications/repetitions events. In these programs, impressive changes of shapes are produced, maintaining the intactness of the original template; new complex structures can be realized through *for*…*in* nested cycles and angle variations; repetitions of a few lines of code mimic TR biological mechanisms: transpositions, frequently occurred during evolution by casual insertions of multiple extra-copies, massive transposon jumps, eventually purified and, if beneficial, conserved by natural selection; TRs increase the probability of duplication and inversion (palindromes) generating new head-to-tail or tail-to-tail TRs. Massive duplications/repetitions events, as those occurred in HOR TR families and in Hox genes (**Figure 7** and **Figure 8**), and currently happening in V(D)J recombination, are simulated by the code of *Recursion vs Iteration* (**Figure 6**). Human antibody and V(D)J biochemistry explain clearly the link between theoretical models, computational codes, and biological pathways: antibody molecules are composed of heavy and light chains, each of which contains both constant (determinism) and variable regions, genetically encoded on different loci; antibody molecules are very resemblant to a population of individuals belonging to the same species, subdivided into some

"*breeds*" (IgA, IgD, IgE, IgG, IgM): millions of different individuals show each one a typical shape; V(D)J recombination rearranges the order of amino acids, changing the tertiary structure of antigen-binding sites, whereas TR rearrangements change the order of monomers, varying the number of cell divisions (size) and their orientations (shape); V(D)J recombination occurs in defined DNA sequences and is operated by specialized enzymes; TR recombinations are controlled and maintained in delimited DNA traits [18] and controlled by similar enzymes [68]; in addition, only some sequences pass the severe evolutionary process of selection. Following this paradigm, the introduced codes suggest how TRs may have reached optimal sequences to encode programs for driving the constant and stable determinism seen in particular developmental stages and the dynamic inter-individual variability to support morphological biodiversity with controlled variance.

5.2. A Possible Evolutionary Mechanism for the Origin of Bilateral Symmetry

Bilateria possess a centrosome comprising two orthogonal centrioles; centrioles are made up of linear tubulin polymers; the centrosome is the unique eukaryotic organelle showing an orthogonal layout. Prokaryotes use a tubulin homolog, the protein FtsZ, that assembles into the Z ring, orthogonal to the longitudinal axis, marking the future division site. Bilateral symmetry is achieved by the orthogonal intersection of two polarity axes, the anterior-posterior and the dorsal-ventral axis [69]. Orthogonality is the main property of bilaterally symmetric systems: e.g., on a 2D plane, symmetric quadrilaterals with orthogonal diagonals (square, rectangle, rhombus) have symmetric sides, but parallelograms, whose diagonals do not intersect orthogonally, are not. From 2d planes to 3D solids, a *z*-axis must be added, orthogonal to the *xy*-plane. These geometrical considerations on biophysical orthogonality suggest centrosomes play a main role in establishing bilateral symmetry in Metazoa. Planarians and other flatworms lack centrosomes: in agreement with the meaning of the words "planarians" and "flatworms", it is almost impossible to build 3D complex structures without a centrosome. [Unlike Bilateria, plants lack centrioles and sagittal plane: sometimes, leaves, petals, or sepals, may appear symmetrical, but careful observations show that veins and edges of leaves, sepals, and petals are only apparently symmetric, also in zygomorphous species as orchids].

Mitotic spindle orientations regulate the positioning of cell division planes during early cleavage divisions, across almost all metazoan: the orientation of first divisions controls the content, position, and fate specification of cells. Spindle positioning is primarily mediated by astral microtubules and cortical polarity cues (which must localize in planned geometrical domains: how is the cell cortex geometrically partitioned into distinguishable compartments?)

Brown and Wolpert [70] hypothesized a chiral "F" molecule, which can be arranged along the anteroposterior and dorsoventral body axes, involved in the

symmetry breaking of the heart, gut, etc.

Bilateria have organs bilaterally symmetric, paired, as Ǝ ∃, D ᗡ, K ꓘ (legs, feet, arms, hands) and unpaired, as A, W, Y, X (cranium, backbone, pelvis, or tongue) besides some asymmetric internal organs: a sagittal plane and a midline are evident in each species. Is it conceivable that so many and so different bilaterally symmetric organs and structures have arisen casually in every species by casual single-point mutations, with the astonishing spatial precision of one cell width [71]? Two different symmetric programs (DNA codes), right and left, in every species and for every organ, cannot have arisen repeatedly, billions and billions of times, produced by chance, adding, step by step, casual single-point mutations. It is impossible that in organisms as different as Arthropods and Vertebrates (different numbers of limbs and appendages, different tissues) an endless number of organs have been perfectly reproduced in their mirror image, always positioned in a correct topographical anatomical location. Moreover, in addition to bilateral symmetry, another major issue concerns centrosomes: the question of multiple axes, *i.e.*, how cells can manage, at the same time, their own reference system, the reference system of the organ they belong to (arms, legs, teeth, feathers) and the reference system of the whole organism. An astonishing example: flight feather follicle cells coordinate the reference system of the whole body, the reference system of the wing, rachis, barb, barbule, besides their intrinsic reference system; in addition, the geometrical pattern of drawings (e.g., peacock) is superimposed: peacock's tail-feathers display symmetrical phyllotaxis patterns, made up of the same number of spirals of adjacent Fibonacci numbers in both, left and right, directions. This overlapping superimposition of different reference systems without any interference makes the function of chemical concentration very difficult if not impossible: morphogen gradients do not operate in 3D in order to control very complex tasks such as the human opposable tumble rotation or the foot-leg angle. Differential equations can model gradients mathematically, but computational simulations of 3D gradient roles in morphogenesis have never been implemented. On the contrary, programs such as *Iter* easily simulate the role of centrosomes in managing multiple reference systems: because of their unique mode of duplication, they maintain the memory of all the previous vectorial additions of axes, *i.e.*, their actual orientation is simply the result of the sum of the precedent vectorial additions (see the program *Iter*, **Figure 1** and the successive orientation of the Python turtle).

As already said, iteration over conserved linear sequences of TRs, together with the geometrical role of centrosomes, is much more accurate than fluctuating morphogen gradients. Do cells possess a tool like a compass? Is the centrosome a sort of chiral cellular compass (dextral/sinistral)? Indeed, because of their peculiar modality of duplication, centrosomes and centrioles can perform complex hierarchical architecture (as in feathers) avoiding the inevitable conflicts of many overlapping molecular gradients. As two individuals equipped with symmetric compasses carry out the same linear code of instructions but travel along two symmet-

rical pathways (**Figure 9**), the emergence, in a common ancestor, of two symmetrical tools able to translate the same genetic linear instructions into two bilaterally symmetric structures is a likely, fast, and simple evolutionary strategy: the difference is inside the tools, not in the coded instructions. The emergence, in a common ancestor, of a simple genetic code for generating (rather, decorating) two symmetrical tools (the centrioles) through a simple mutation is implemented in the codes of the programs *Morphogenesis*, *Bilateral Symmetry* and *Iter*; in these programs, only one byte of code (a minus sign, "–") produces two enantiomorph tools (Python turtles) that, in turn, use the same linear program for creating left- and right-handed graphics. Is a similar event possible in biological systems?

The centrosome is a membrane-less organelle made up of two orthogonal centrioles; centrioles show a typical 9-fold symmetry, whose quaternary structure is founded on the SAS-6 protein; SAS-6 builds regular polymers of nine sides (**Figure 10**) connected at 140˚: SAS-6 monomers face central angles of 40˚, defined "centriolar angle" in Materials and Methods, [72] [73]. The rotational asymmetry of centrioles and cilia basal bodies has been studied in Protists: their nine triplets, assembled in a defined and sorted sequence, are non-equivalent; circumferential polarity has been confirmed from ciliates to mammals [30] [74]-[79]. The centrosome is wired to the cell membrane by an aster of microtubules (see: Satir: *Chirality of the cytoskeleton in the origin of cellular symmetry* [21]): centrosome structure and its unique process of duplication [80] suggest it is the cellular geometry organizer, whose orientation relative to the sagittal plane of the whole organism is maintained and transmitted from parent to descendant cells by the mechanism of spindle orientation and spindle pole positioning during mitosis. In the program *Iter* the instruction *sat_DNA.pop*(*0*), quite similar to the successive geographic instructions of **Figure 9**, takes, step by step, the programmed value of the angle that will orient the spindle axis, simulating how TRs can be the linear DNA code for programmed oriented cell divisions.

Assembled in the zygote and inherited by the two first blastomeres, the two chiral centrosomes generate (and transmit to offspring) chiral cytoskeletons (actin, microtubules, cortical domains): following a unique developmental code, they assemble pairs of bilaterally symmetric structures. In the attached programs, it has been assumed that astral microtubules, irradiating from the centrosome towards the cell membrane, are responsible for the chirality of the cytoskeleton [21]: microtubules, used as tracks by dynein and kinesin to carry materials, to be distinguishable must be labeled by molecular-geometrical markers, corresponding to their spatial direction: this assertion is a theoretical requirement of mechanobiology (topology of metric spaces). Thus, the programs reproduce the highly geometric disposition of blastomeres during early cleavage: in radial, spiral, bilateral, and rotational holoblastic [81] [82] embryos show an invariant, bilaterally symmetric, division pattern up to gastrulation: spindle orientation and division timing are strictly predictable.

Because the zygote inherits only one functional centriole, the second centriole of the zygote, in the introduced programs, is assumed to have been assembled

bilaterally symmetric, relative to the inherited sperm centriole: so, during the cleavage, independent from signals like gravity or light, but strictly tied to the initial orientation of the zygote poles, the mother chiral centrioles of the first blastomeres follow a coordinated and ordered (coded) sequence of instructions for the 3D spatial positionings of the spindle poles; mitosis after mitosis, mother centrioles attentively transmit and share their chiral reference system to descendant cells (besides the common general reference system of the whole organism) through the peculiar duplication mechanisms of centriole and centrosome duplication: this is an essential process of mechanobiology to keep memory of the whole body sagittal plane position and share progenitor's cytoskeletal polarization (nothing else than a simple sequential vectorial addition); eventually, planar cell polarity components and extracellular matrix fibers orientation coordinate a large number of cells in tissues. Some questions: how is planar cell polarity component and extracellular matrix fiber geometry organized? Does planar polarity operate in parallel to cell chirality (or even downstream)? As demonstrated in planarian epidermis, are tissues first patterned bilaterally symmetric by cellular chiral components [22]?

In the program *Iter*, the nine, non-equivalent centriolar triplets are supposed to have been previously labeled by nine different receptors: the program uses short TR DNA sequences, similar but not identical, each one carrying angle information and used as a signal capable of recognizing only one triplet (as in codon/anticodon matching) to perform the correct cortical location of the spindle poles: a possible code system for nine centriolar angles, similar to the codon/anticodon system for distinguishing and recognizing amino acids, has been hypothesized. Several studies have found that noncoding RNAs support as scaffolds the structure of subcellular membrane-less organelles like the centrosome [83]. In addition, many not coding RNAs localize to the centrosome [84]: they can decorate different MTOCs (MicroTubule-Organizing Center) and γ-TuRCs (γ-Tubulin Ring Complex), by labeling them with molecular-geometrical markers corresponding to their 3D position on the centrosome (inherited, shared, issued and established through the peculiar centriole duplication mechanism) and to the direction of the microtubules they nucleate. Notably, SAS-6 self-assembles into 9-fold radially symmetric ring-shaped oligomers to form the cartwheel, a structure critical for building the centriole: crystallographic structures of the single-cell green alga *Chlamydomonas reinhardtii* suggest that SAS-6 coiled-coil complexes interact asymmetrically, thereby imparting polarity to the cartwheel [85] [86].

Enantiomorph molecules generate enantiomorph crystals, right- and left-handed, as quartz: live images by Ferreira *et al.* [54] show that in the zebrafish Kupffer's vesicle (the left-right organizer, homologous of the chick Hensen's node) cilia are asymmetrically oriented in the right and left sides: primary cilia (and their centriole/basal bodies) possess a real chiral "static" scaffolding, not a simply chiral "dynamic" rotation [30]. The nine centriolar non-equivalent triplets are assembled in a defined and sorted sequence [53] [54], resulting in a defined rotational asymmetry. Alliegro [87] identified 36 different centrosomal RNAs: it

is conceivable that a circular ribonucleoprotein drives the correct rotational polarization of centrioles and that, through a reverse transposition of its beginning trait [88] [89] a new flipped (swapped) not coding RNA emerged (**Figure 11**): reverse duplications are quite frequent in the transposition of TRs because of their big palindromic clusters; two flipped lncRNAs may easily reverse, in turn, the rotational polarity of the centriole (as in the compasses of the previous thought experiment), generating two enantiomorph centrioles [30] [74]-[79] [86]-[94]. In *Morphogenesis* two bilaterally symmetric complex structures are generated: the midline is intentionally crossed in three positions, like pyramidal decussation or optic chiasma in many vertebrates, (**Figure 1**, **Figure 2**, **Figure 4**): the instruction "*forward*" reproduces the process of cell division without changing the orientation of the last division plane, whereas instructions like "*left*(θ˚)" and "*right*(θ˚)" simulate a programmed change of direction. In these programs, enantiomorph centrioles and centrosomes act as geometrical organizers to realize bilaterally symmetric structures, decoding DNA geometric instructions.

Following this paradigm, in *Morphogenesis* and *Iter* (**Figures 3-5**) only one code byte (a minus sign, "–") produces two enantiomorph tools that use a unique program for both left and right drawings.

6. Conclusions

This study is a pioneering attempt to ascertain, in the evolution of complex organs, the suggested role of TRs in counting cell divisions and the centrosome's role in translating genetic codes into correct 3D spatially planned directions.

The most rational hypothesis, relying on logical perspectives, to explain how TRs may function as facilitators of evolution, enabling extremely rapid evolution of new forms is that TRs are iterated to count cell divisions: well-conserved TRs manage deterministic characters, while TR variability manages the last developmental stages; they regulating the final number of cells in organs of different breeds, resulting, for example, in variable lengths of legs, tails or ears.

Monomers responsible for the orientation of the division plane may form long sequences of TRs: these TRs are the genomic codes for arranging cells in geometrical dispositions; they are subject to DNA changes, which is common in TRs: during evolution, the order of monomers in a sequence may have been remodeled and rearranged, causing the emergence of new shapes. Because of the described capability of managing both the number of cell divisions and the growth directions, TRs may be responsible for the rapid emergence of new phenotypes described in dog breeds.

Further research (already started) should be conducted to find and understand hidden structures in DNA through power algorithms such as 1D Convolutional and Recurrent Neural Networks.

Conflicts of Interest

The author declares no conflicts of interest regarding the publication of this paper.

References

[1] Laland, K., Uller, T., Feldman, M., Sterelny, K., Müller, G.B., Moczek, A., *et al.* (2014) Does Evolutionary Theory Need a Rethink? *Nature*, **514**, 161-164. https://doi.org/10.1038/514161a

[2] Andersen, J.S., Wilkinson, C.J., Mayor, T., Mortensen, P., Nigg, E.A. and Mann, M. (2003) Proteomic Characterization of the Human Centrosome by Protein Correlation Profiling. *Nature*, **426**, 570-574. https://doi.org/10.1038/nature02166

[3] Myers, P. (2007) Tandem Repeats and Morphological Variation. *Nature Education*, **1**, 1.

[4] Ostrander, E.A. (2007) Genetics and the Shape of Dogs. *American Scientist*, **95**, 406. https://doi.org/10.1511/2007.67.406

[5] Fondon, J.W. and Garner, H.R. (2004) Molecular Origins of Rapid and Continuous Morphological Evolution. *Proceedings of the National Academy of Sciences of the United States of America*, **101**, 18058-18063. https://doi.org/10.1073/pnas.0408118101

[6] Sears, K.E., Goswami, A., Flynn, J.J. and Niswander, L.A. (2007) The Correlated Evolution of *runx2* Tandem Repeats, Transcriptional Activity, and Facial Length in Carnivora. *Evolution & Development*, **9**, 555-565. https://doi.org/10.1111/j.1525-142x.2007.00196.x

[7] Balzano, E., Pelliccia, F. and Giunta, S. (2021) Genome (In)stability at Tandem Repeats. *Seminars in Cell & Developmental Biology*, **113**, 97-112. https://doi.org/10.1016/j.semcdb.2020.10.003

[8] Wahls, W.P., Wallace, L.J. and Moore, P.D. (1990) Hypervariable Minisatellite DNA Is a Hotspot for Homologous Recombination in Human Cells. *Cell*, **60**, 95-103. https://doi.org/10.1016/0092-8674(90)90719-u

[9] Ruiz-Ruano, F.J., López-León, M.D., Cabrero, J. and Camacho, J.P.M. (2016) High-throughput Analysis of the Satellitome Illuminates Satellite DNA Evolution. *Scientific Reports*, **6**, Article No. 28333. https://doi.org/10.1038/srep28333

[10] Cacheux, L., Ponger, L., Gerbault-Seureau, M., Richard, F.A. and Escudé, C. (2016) Diversity and Distribution of *α* Satellite DNA in the Genome of an Old World Monkey: *Cercopithecus solatus*. *BMC Genomics*, **17**, Article No. 916. https://doi.org/10.1186/s12864-016-3246-5

[11] Ahmad, S.F., Singchat, W., Jehangir, M., Suntronpong, A., Panthum, T., Malaivijitnond, S., *et al.* (2020) Dark Matter of Primate Genomes: Satellite DNA Repeats and Their Evolutionary Dynamics. *Cells*, **9**, Article 2714. https://doi.org/10.3390/cells9122714

[12] Ma, S., Skarica, M., Li, Q., Xu, C., Risgaard, R.D., Tebbenkamp, A.T.N., *et al.* (2022) Molecular and Cellular Evolution of the Primate Dorsolateral Prefrontal Cortex. *Science*, **377**, eabo7257. https://doi.org/10.1126/science.abo7257

[13] Sun, F., Fleurdépine, S., Bousquet-Antonelli, C., Caetano-Anollés, G. and Deragon, J. (2007) Common Evolutionary Trends for SINE RNA Structures. *Trends in Genetics*, **23**, 26-33. https://doi.org/10.1016/j.tig.2006.11.005

[14] Malgrange, B. and Nguyen, L. (2022) Scaling Brain Neurogenesis across Evolution. *Science*, **377**, 1155-1156. https://doi.org/10.1126/science.ade4388

[15] Regolini, M.F.G. (2024) DNA Tandem Repeats as Iterable Objects to Count Cell Divisions: A Computational Model. *Advances in Bioscience and Biotechnology*, **15**, 207-234. https://doi.org/10.4236/abb.2024.154015

[16] Brown, R.E. and Freudenreich, C.H. (2021) Structure-forming Repeats and Their Impact on Genome Stability. *Current Opinion in Genetics & Development*, **67**, 41-51. https://doi.org/10.1016/j.gde.2020.10.006

[17] Shi, G., Pang, Q., Lin, Z., Zhang, X. and Huang, K. (2024) Repetitive Sequence Stability in Embryonic Stem Cells. *International Journal of Molecular Sciences*, **25**, Article 8819. https://doi.org/10.3390/ijms25168819

[18] Schaper, E., Gascuel, O. and Anisimova, M. (2014) Deep Conservation of Human Protein Tandem Repeats within the Eukaryotes. *Molecular Biology and Evolution*, **31**, 1132-1148. https://doi.org/10.1093/molbev/msu062

[19] Fedorov, A.N., Fedorova, L.V., Grechko, V.V., Ryabinin, D.M., Sheremet'eva, V.A., Bannikova, A.A., *et al.* (1999) Variable and Invariable DNA Repeat Characters Revealed by Taxonprint Approach Are Useful for Molecular Systematics. *Journal of Molecular Evolution*, **48**, 69-76. https://doi.org/10.1007/pl00006446

[20] Gilbert S.F. and Barresi M.J.F. (2016) Developmental Biology. 7th Edition, Sinauer Associates.

[21] Satir, P. (2016) Chirality of the Cytoskeleton in the Origins of Cellular Asymmetry. *Philosophical Transactions of the Royal Society B: Biological Sciences*, **371**, Article ID: 20150408. https://doi.org/10.1098/rstb.2015.0408

[22] Basquin, C., Ershov, D., Gaudin, N., Vu, H.T., Louis, B., Papon, J., *et al.* (2019) Emergence of a Bilaterally Symmetric Pattern from Chiral Components in the Planarian Epidermis. *Developmental Cell*, **51**, 516-525.e5. https://doi.org/10.1016/j.devcel.2019.10.021

[23] Rahman, T., Peters, F.D. and Wan, L.Q. (2024) Biomechanical Modeling of Cell Chirality and Symmetry Breaking of Biological Systems. *Mechanobiology in Medicine*, **2**, Article ID: 100038. https://doi.org/10.1016/j.mbm.2024.100038

[24] Marshall, W.F. (2012) Centriole Asymmetry Determines Algal Cell Geometry. *Current Opinion in Plant Biology*, **15**, 632-637. https://doi.org/10.1016/j.pbi.2012.09.011

[25] Regolini, M. (2014) Centrosome, Cell Geometry and Tissue Topology. The Biological 3D Reference System of Metazoa. *International Journal of Current Research*, **6**, 9685-9689.

[26] Olivier, B.G., Rohwer, J.M. and Hofmeyr, J.S. (2002) Modelling Cellular Processes With Python and Scipy. *Molecular Biology Reports*, **29**, 249-254. https://doi.org/10.1023/a:1020346417223

[27] Tomás, H. (2011) Boolean Modeling of Biochemical Networks. *The Open Bioinformatics Journal*, **5**, 16-25. https://doi.org/10.2174/1875036201105010016

[28] Chiang, C., Ohashi, M. and Tang, Y. (2023) Deciphering Chemical Logic of Fungal Natural Product Biosynthesis through Heterologous Expression and Genome Mining. *Natural Product Reports*, **40**, 89-127. https://doi.org/10.1039/d2np00050d

[29] Boniolo, G., D'Agostino, M., Piazza, M. and Pulcini, G. (2021) Molecular Biology Meets Logic: Context-Sensitiveness in Focus. *Foundations of Science*, **28**, 307-325. https://doi.org/10.1007/s10699-021-09789-y

[30] Gaudin, N., Martin Gil, P., Boumendjel, M., Ershov, D., Pioche-Durieu, C., Bouix, M., *et al.* (2022) Evolutionary Conservation of Centriole Rotational Asymmetry in the Human Centrosome. *eLife*, **11**, e72382. https://doi.org/10.7554/elife.72382

[31] Burmeister, A.R. (2015) Horizontal Gene Transfer: Figure 1. *Evolution, Medicine, and Public Health*, **2015**, 193-194. https://doi.org/10.1093/emph/eov018

[32] Avni, E. and Snir, S. (2020) A New Phylogenomic Approach for Quantifying Horizontal Gene Transfer Trends in Prokaryotes. *Scientific Reports*, **10**, Article No. 12425. https://doi.org/10.1038/s41598-020-62446-5

[33] Shabbir, M.A.B., Hao, H., Shabbir, M.Z., Wu, Q., Sattar, A. and Yuan, Z. (2016) Bacteria vs. Bacteriophages: Parallel Evolution of Immune Arsenals. *Frontiers in Microbiology*, **7**, Article 1292. https://doi.org/10.3389/fmicb.2016.01292

[34] Pray, L. (2008) DNA Replication and Causes of Mutation. *Nature Education*, **1**, 214.

[35] Katsonis, P., Koire, A., Wilson, S.J., Hsu, T., Lua, R.C., Wilkins, A.D., *et al.* (2014) Single Nucleotide Variations: Biological Impact and Theoretical Interpretation. *Protein Science*, **23**, 1650-1666. https://doi.org/10.1002/pro.2552

[36] Barton, R.A. and Venditti, C. (2014) Rapid Evolution of the Cerebellum in Humans and Other Great Apes. *Current Biology*, **24**, 2440-2444. https://doi.org/10.1016/j.cub.2014.08.056

[37] Zhuang, X., Shao, Y., Chen, C., Zhou, L., Yao, Y., Cooper, D.N., *et al.* (2024) Divergent Evolutionary Rates of Primate Brain Regions as Revealed by Genomics and Transcriptomics. *Genome Biology and Evolution*, **16**, evae023. https://doi.org/10.1093/gbe/evae023

[38] Fan, H. and Chu, J. (2007) A Brief Review of Short Tandem Repeat Mutation. *Genomics, Proteomics & Bioinformatics*, **5**, 7-14. https://doi.org/10.1016/s1672-0229(07)60009-6

[39] Gemayel, R., Cho, J., Boeynaems, S. and Verstrepen, K.J. (2012) Beyond Junk-Variable Tandem Repeats as Facilitators of Rapid Evolution of Regulatory and Coding Sequences. *Genes*, **3**, 461-480. https://doi.org/10.3390/genes3030461

[40] Dogan, M., Pouch, M., Mandáková, T., Hloušková, P., Guo, X., Winter, P., *et al.* (2022) Corrigendum: Evolution of Tandem Repeats Is Mirroring Post-Polyploid Cladogenesis in *Heliophila* (Brassicaceae). *Frontiers in Plant Science*, **13**, Article 1054800. https://doi.org/10.3389/fpls.2022.1054800

[41] Beauregard, A., Curcio, M.J. and Belfort, M. (2008) The Take and Give between Retrotransposable Elements and Their Hosts. *Annual Review of Genetics*, **42**, 587-617. https://doi.org/10.1146/annurev.genet.42.110807.091549

[42] Vassetzky, N.S. and Kramerov, D.A. (2012) SINEBase: A Database and Tool for SINE Analysis. *Nucleic Acids Research*, **41**, D83-D89. https://doi.org/10.1093/nar/gks1263

[43] Ishak, C.A. and De Carvalho, D.D. (2020) Reactivation of Endogenous Retroelements in Cancer Development and Therapy. *Annual Review of Cancer Biology*, **4**, 159-176. https://doi.org/10.1146/annurev-cancerbio-030419-033525

[44] Sharma, A., Wolfgruber, T.K. and Presting, G.G. (2013) Tandem Repeats Derived from Centromeric Retrotransposons. *BMC Genomics*, **14**, Article No. 142. https://doi.org/10.1186/1471-2164-14-142

[45] Paço, A., Freitas, R. and Vieira-da-Silva, A. (2019) Conversion of DNA Sequences: From a Transposable Element to a Tandem Repeat or to a Gene. *Genes*, **10**, Article 1014. https://doi.org/10.3390/genes10121014

[46] Wang, W. and Kirkness, E.F. (2005) Short Interspersed Elements (SINEs) Are a Major Source of Canine Genomic Diversity. *Genome Research*, **15**, 1798-1808. https://doi.org/10.1101/gr.3765505

[47] Böhne, A., Brunet, F., Galiana-Arnoux, D., Schultheis, C. and Volff, J. (2008) Transposable Elements as Drivers of Genomic and Biological Diversity in Vertebrates. *Chromosome Research*, **16**, 203-215. https://doi.org/10.1007/s10577-007-1202-6

[48] Zhang, Y., Hu, N., Xu, J. and Wang, Z. (2023) DNA Logic Programming: From Con-

cept to Construction. *VIEW*, **5**, Article ID: 20230062. https://doi.org/10.1002/viw.20230062

[49] Black, E.M. and Giunta, S. (2018) Repetitive Fragile Sites: Centromere Satellite DNA as a Source of Genome Instability in Human Diseases. *Genes*, **9**, Article 615. https://doi.org/10.3390/genes9120615

[50] Ahmed, M. and Liang, P. (2012) Transposable Elements Are a Significant Contributor to Tandem Repeats in the Human Genome. *Comparative and Functional Genomics*, **2012**, Article ID: 947089. https://doi.org/10.1155/2012/947089

[51] Zattera, M.L. and Bruschi, D.P. (2022) Transposable Elements as a Source of Novel Repetitive DNA in the Eukaryote Genome. *Cells*, **11**, Article 3373. https://doi.org/10.3390/cells11213373

[52] McGurk, M.P. and Barbash, D.A. (2018) Double Insertion of Transposable Elements Provides a Substrate for the Evolution of Satellite DNA. *Genome Research*, **28**, 714-725. https://doi.org/10.1101/gr.231472.117

[53] Guichard, P., Hachet, V., Majubu, N., Neves, A., Demurtas, D., Olieric, N., *et al.* (2013) Native Architecture of the Centriole Proximal Region Reveals Features Underlying Its 9-Fold Radial Symmetry. *Current Biology*, **23**, 1620-1628. https://doi.org/10.1016/j.cub.2013.06.061

[54] Ferreira, R.R., Pakula, G., Klaeyle, L., Fukui, H., Vilfan, A., Supatto, W., *et al.* (2018) Chiral Cilia Orientation in the Left-Right Organizer. *Cell Reports*, **25**, 2008-2016.e4. https://doi.org/10.1016/j.celrep.2018.10.069

[55] Regolini, M. (2019) The Centrosome as a Geometry Organizer. In: Kloc, M., Ed., *The Golgi Apparatus and Centriole*, Springer, 253-276. https://doi.org/10.1007/978-3-030-23173-6_11

[56] Laporte, M. (2024) Time-Series Reconstruction of the Molecular Architecture of human Centriole Assembly. *Cell*, **187**, 2158-2174.e19.

[57] LeGuennec, M., Klena, N., Aeschlimann, G., Hamel, V. and Guichard, P. (2021) Overview of the Centriole Architecture. *Current Opinion in Structural Biology*, **66**, 58-65. https://doi.org/10.1016/j.sbi.2020.09.015

[58] Nazarov, S., Bezler, A., Hatzopoulos, G.N., Nemčíková Villímová, V., Demurtas, D., Le Guennec, M., *et al.* (2020) Novel Features of Centriole Polarity and Cartwheel Stacking Revealed by Cryo-Tomography. *The EMBO Journal*, **39**, e106249. https://doi.org/10.15252/embj.2020106249

[59] Woglar, A., Pierron, M., Schneider, F.Z., Jha, K., Busso, C. and Gönczy, P. (2022) Molecular Architecture of the *C. elegans* Centriole. *PLOS Biology*, **20**, e3001784. https://doi.org/10.1371/journal.pbio.3001784

[60] Fishman, E.L., Jo, K., Nguyen, Q.P.H., Kong, D., Royfman, R., Cekic, A.R., *et al.* (2018) Author Correction: A Novel Atypical Sperm Centriole Is Functional during Human Fertilization. *Nature Communications*, **9**, Article No. 2800. https://doi.org/10.1038/s41467-018-05324-z

[61] Avidor-Reiss, T. (2018) Rapid Evolution of Sperm Produces Diverse Centriole Structures That Reveal the Most Rudimentary Structure Needed for Function. *Cells*, **7**, Article 67. https://doi.org/10.3390/cells7070067

[62] Regolini, M. (2015) Centrosome RNA: A Molecular Basis for Non-Equivalence of Triplets in Centrioles and Centrosomes. *Molecular Biology*, **4**, Article ID: 1000125.

[63] Axelrod, J.D. (2020) Planar Cell Polarity Signaling in the Development of Left-Right Asymmetry. *Current Opinion in Cell Biology*, **62**, 61-69. https://doi.org/10.1016/j.ceb.2019.09.002

[64] Conceição, I.C., Long, A.D., Gruber, J.D. and Beldade, P. (2011) Genomic Sequence around Butterfly Wing Development Genes: Annotation and Comparative Analysis. *PLOS ONE*, **6**, e23778. https://doi.org/10.1371/journal.pone.0023778

[65] Jiggins, C.D., Wallbank, R.W.R. and Hanly, J.J. (2017) Waiting in the Wings: What Can We Learn about Gene Co-Option from the Diversification of Butterfly Wing Patterns? *Philosophical Transactions of the Royal Society B: Biological Sciences*, **372**, 20150485. https://doi.org/10.1098/rstb.2015.0485

[66] Mazo-Vargas, A., Langmüller, A.M., Wilder, A., van der Burg, K.R.L., Lewis, J.J., Messer, P.W., *et al.* (2022) Deep Cis-Regulatory Homology of the Butterfly Wing Pattern Ground Plan. *Science*, **378**, 304-308. https://doi.org/10.1126/science.abi9407

[67] Lower, S.S., McGurk, M.P., Clark, A.G. and Barbash, D.A. (2018) Satellite DNA Evolution: Old Ideas, New Approaches. *Current Opinion in Genetics & Development*, **49**, 70-78. https://doi.org/10.1016/j.gde.2018.03.003

[68] Durrant, M.G., Perry, N.T., Pai, J.J., Jangid, A.R., Athukoralage, J.S., Hiraizumi, M., *et al.* (2024) Bridge RNAs Direct Programmable Recombination of Target and Donor DNA. *Nature*, **630**, 984-993. https://doi.org/10.1038/s41586-024-07552-4

[69] Finnerty, J.R. (2003) The Origins of Axial Patterning in the Metazoa: How Old Is Bilateral Symmetry? *The International Journal of Developmental Biology*, **47**, 523-529.

[70] Brown, N.A. and Wolpert, L. (1990) The Development of Handedness in Left/Right Asymmetry. *Development*, **109**, 1-9. https://doi.org/10.1242/dev.109.1.1

[71] Abouchar, L., Petkova, M.D., Steinhardt, C.R. and Gregor, T. (2014) Fly Wing Vein Patterns Have Spatial Reproducibility of a Single Cell. *Journal of the Royal Society Interface*, **11**, Article ID: 20140443. https://doi.org/10.1098/rsif.2014.0443

[72] Gopalakrishnan, J., Guichard, P., Smith, A.H., Schwarz, H., Agard, D.A., Marco, S., *et al.* (2010) Self-Assembling SAS-6 Multimer Is a Core Centriole Building Block. *Journal of Biological Chemistry*, **285**, 8759-8770. https://doi.org/10.1074/jbc.m109.092627

[73] Ford, J., Stansfeld, P. and Vakonakis, I. (2017) Coupling Form and Function: How the Oligomerisation Symmetry of the SAS-6 Protein Contributes to the Architecture of Centriole Organelles. *Symmetry*, **9**, Article 74. https://doi.org/10.3390/sym9050074

[74] Beisson, J. and Jerka-Dziadosz, M. (1999) Polarities of the Centriolar Structure: Morphogenetic Consequences. *Biology of the Cell*, **91**, 367-378. https://doi.org/10.1111/j.1768-322x.1999.tb01094.x

[75] Bengueddach, H., Lemullois, M., Aubusson-Fleury, A. and Koll, F. (2017) Basal Body Positioning and Anchoring in the Multiciliated Cell *Paramecium tetraurelia*: Roles of OFD1 and VFL3. *Cilia*, **6**, Article No. 6. https://doi.org/10.1186/s13630-017-0050-z

[76] Geimer, S. and Melkonian, M. (2004) The Ultrastructure of The *Chlamydomonas reinhardtii* Basal Apparatus: Identification of an Early Marker of Radial Asymmetry Inherent in the Basal Body. *Journal of Cell Science*, **117**, 2663-2674. https://doi.org/10.1242/jcs.01120

[77] Pearson, C.G. and Winey, M. (2009) Basal Body Assembly in Ciliates: The Power of Numbers. *Traffic*, **10**, 461-471. https://doi.org/10.1111/j.1600-0854.2009.00885.x

[78] Regolini, M. (2019) Centrosome: Is It a Geometric, Noise Resistant, 3D Interface That Translates Morphogenetic Signals into Precise Locations in the Cell? *Italian Journal of Anatomy and Embryology*, **118**, 19-66.

[79] Regolini, M. (2019) Centriole Enantiomerism: Unexpected Information from Mice and Fish. *Italian Journal of Anatomy and Embryology*, **123**, 232-240.

[80] Fu, J., Hagan, I.M. and Glover, D.M. (2015) The Centrosome and Its Duplication Cycle. *Cold Spring Harbor Perspectives in Biology*, **7**, a015800. https://doi.org/10.1101/cshperspect.a015800

[81] Abe, M., Takahashi, H. and Kuroda, R. (2014) Spiral Cleavages Determine the Left-Right Body Plan by Regulating Nodal Pathway in Monomorphic Gastropods, *Physa acuta*. *The International Journal of Developmental Biology*, **58**, 513-520. https://doi.org/10.1387/ijdb.140087rk

[82] Martín-Durán, J.M. and Marlétaz, F. (2020) Unravelling Spiral Cleavage. *Development*, **147**, dev181081. https://doi.org/10.1242/dev.181081

[83] Ito, K.K., Watanabe, K. and Kitagawa, D. (2020) The Emerging Role of ncRNAs and RNA-Binding Proteins in Mitotic Apparatus Formation. *Non-Coding RNA*, **6**, Article 13. https://doi.org/10.3390/ncrna6010013

[84] Ishigaki, Y., Nakamura, Y., Tatsuno, T., Hashimoto, M., Iwabuchi, K. and Tomosugi, N. (2013) RNA-binding Protein RBM8A (Y14) and MAGOH Localize to Centrosome in Human A549 Cells. *Histochemistry and Cell Biology*, **141**, 101-109. https://doi.org/10.1007/s00418-013-1135-4

[85] Kantsadi, A.L., Hatzopoulos, G.N., Gönczy, P. and Vakonakis, I. (2022) Structures of SAS-6 Coiled Coil Hold Implications for the Polarity of the Centriolar Cartwheel. *Structure*, **30**, 671-684.e5. https://doi.org/10.1016/j.str.2022.02.005

[86] Gupta, A. and Kitagawa, D. (2018) Ultrastructural Diversity between Centrioles of Eukaryotes. *The Journal of Biochemistry*, **164**, 1-8. https://doi.org/10.1093/jb/mvy031

[87] Alliegro, M.C. and Alliegro, M.A. (2008) Centrosomal RNA Correlates with Intron-Poor Nuclear Genes in *Spisula* Oocytes. *Proceedings of the National Academy of Sciences of the United States of America*, **105**, 6993-6997. https://doi.org/10.1073/pnas.0802293105

[88] Alliegro, M.C., Alliegro, M.A. and Palazzo, R.E. (2006) Centrosome-Associated RNA in Surf Clam Oocytes. *Proceedings of the National Academy of Sciences of the United States of America*, **103**, 9034-9038. https://doi.org/10.1073/pnas.0602859103

[89] Chichinadze, K., Lazarashvili, A. and Tkemaladze, J. (2012) RNA in Centrosomes: Structure and Possible Functions. *Protoplasma*, **250**, 397-405. https://doi.org/10.1007/s00709-012-0422-6

[90] Barvitenko, N., Lawen, A., Aslam, M., Pantaleo, A., Saldanha, C., Skverchinskaya, E., *et al.* (2018) Integration of Intracellular Signaling: Biological Analogues of Wires, Processors and Memories Organized by a Centrosome 3D Reference System. *Biosystems*, **173**, 191-206. https://doi.org/10.1016/j.biosystems.2018.08.007

[91] Fry, A.M., Sampson, J., Shak, C. and Shackleton, S. (2017) Recent Advances in Pericentriolar Material Organization: Ordered Layers and Scaffolding Gels. *F*1000*Research*, **6**, Article 1622. https://doi.org/10.12688/f1000research.11652.1

[92] Panda, S., Setia, M., Kaur, N., Shepal, V., Arora, V., Singh, D.K., *et al.* (2018) Noncoding RNA Ginir Functions as an Oncogene by Associating with Centrosomal Proteins. *PLOS Biology*, **16**, e2004204. https://doi.org/10.1371/journal.pbio.2004204

[93] Bayless, B.A., Galati, D.F. and Pearson, C.G. (2015) *Tetrahymena* Basal Bodies. *Cilia*, **5**, Article No. 1. https://doi.org/10.1186/s13630-016-0022-8

[94] Beisson, J. and Sonneborn, T.M. (1965) Cytoplasmic Inheritance of the Organization of the Cell Cortex in Paramecium Aurelia. *Proceedings of the National Academy of Sciences of the United States of America*, **53**, 275-282. https://doi.org/10.1073/pnas.53.2.275

Abbreviations

TR	Tandem Repeat
TE	Transposable Element